

ANL-6719  
RETURN TO IDAHO LIBRARY

# Argonne National Laboratory

## PHYSICS DIVISION SUMMARY REPORT

March-May 1963

### LEGAL NOTICE

*This report was prepared as an account of Government sponsored work. Neither the United States, nor the Commission, nor any person acting on behalf of the Commission:*

- A. Makes any warranty or representation, expressed or implied, with respect to the accuracy, completeness, or usefulness of the information contained in this report, or that the use of any information, apparatus, method, or process disclosed in this report may not infringe privately owned rights; or*
- B. Assumes any liabilities with respect to the use of, or for damages resulting from the use of any information, apparatus, method, or process disclosed in this report.*

*As used in the above, "person acting on behalf of the Commission" includes any employee or contractor of the Commission, or employee of such contractor, to the extent that such employee or contractor of the Commission, or employee of such contractor prepares, disseminates, or provides access to, any information pursuant to his employment or contract with the Commission, or his employment with such contractor.*

ARGONNE NATIONAL LABORATORY  
9700 South Cass Avenue  
Argonne, Illinois

PHYSICS DIVISION  
SUMMARY REPORT

March-May 1963

Lowell M. Bollinger, Division Director

Preceding Summary Reports:

ANL-6612, September-October 1962  
ANL-6666, November-December 1962  
ANL-6679, January-February 1963

Operated by The University of Chicago  
under  
Contract W-31-109-eng-38  
with the  
U. S. Atomic Energy Commission





## FOREWORD

The Summary Report of the Physics Division of the Argonne National Laboratory is issued monthly for the information of the members of the Division and a limited number of other persons interested in the progress of the work. Each active project reports about once in 3 months, on the average. Those not reported in a particular issue are listed separately in the Table of Contents with a reference to the last issue in which each appeared.

This is merely an informal progress report. The results and data therefore must be understood to be preliminary and tentative.

The issuance of these reports is not intended to constitute publication in any sense of the word. Final results either will be submitted for publication in regular professional journals or, in special cases, will be presented in ANL Topical Reports.



## TABLE OF CONTENTS

The date of the last preceding report is indicated after the title of each project below. Active projects that are not reported in this issue are listed on subsequent pages.

### PAGE

#### I. EXPERIMENTAL NUCLEAR PHYSICS

I-6-1	DOUBLE ISOMERISM IN $\text{As}^{73}$ (New project)  H. H. Bolotin . . . . .	1
	The levels in $\text{As}^{73}$ , populated by the decay of $\text{Se}^{73}$ , were studied. States at 0.425 and 0.066 MeV were found to decay by means of two cascade gamma rays with energies of 0.359 and 0.066 MeV, with no observed cross-over transition. Half-lives of $5.0 \pm 0.4 \mu\text{sec}$ and $6.1 \pm 0.4 \text{ nsec}$ were measured for the 0.425- and 0.066-MeV states, respectively. The 0.066-MeV transition, previously assigned as M1, was found to be retarded by a factor of 97 compared to single-particle estimates. This result tends to confirm the $\ell$ -forbidden character of this transition. This retardation is compared with that for the 0.068-MeV transition in $\text{Ni}^{61}$ which proceeds between analogous states.	
I-9-4	LIFETIMES OF ENERGY LEVELS EXCITED BY SLOW-NEUTRON CAPTURE (ANL-6326, March 1961)  H. H. Bolotin . . . . .	7
	A program has been initiated to investigate low-lying excited states which are populated by slow-neutron capture and subsequent $\gamma$ -ray decay. The object of this series of investigations is to determine, where feasible, the lifetimes of these levels, and to obtain as much additional information as possible about these levels and the transitions proceeding from them. An outline and description of the experimental methods are presented.	

I-21-11      EXCITED STATES OF LIGHT NUCLEI  
(ANL-6679, January-February 1963)

R. G. Allas, S. S. Hanna, L. S. Meyer,  
and R. E. Segel . . . . . 10

The gamma radiation following the capture of protons by  $B^{11}$  has been extensively studied in the energy region  $E_p = 4-10$  MeV, the region of the giant resonance in  $C^{12}$ . The work is part of a program to systematically study the capture of protons into the giant resonance.

I-50-1      SEARCH FOR A PARTICLE-STABLE TETRA  
NEUTRON (New project)

J. P. Schiffer and R. Vandenbosch (CHM). . . . . 13

A search for particle-stable tetra neutrons and di neutrons in fission revealed that they occur with a frequency of less than  $5 \times 10^{-9}$  per fission.

I-55-13      CAPTURE GAMMA-RAY SPECTRA FOR NEU-  
TRONS WITH ENERGIES FROM 0.1 TO 10 EV  
(ANL-6679, January-February 1963)

S. Raboy and C. C. Trail . . . . . 17

The neutron capture cross section for deuterium has been measured relative to hydrogen by observing the relative intensities of the gamma rays emitted by the two nuclei. The capture cross section for deuterium is found to be  $362 \pm 26 \mu b$ .

## II. MASS SPECTROSCOPY

II-23-2      SPUTTERING EXPERIMENTS IN THE RUTHER-  
FORD COLLISION REGION (ANL-6488, January  
1962)

M. S. Kaminsky . . . . . 25

The existence of preferred ejection directions in the back sputtering of particles from a Cu(100)

plane under deuteron bombardment has been established for the Rutherford collision region. The data are compared with recently developed theories of cascades of focused collision sequences in the lattices of metal monocrystals.

## V. THEORETICAL PHYSICS, GENERAL

- V-49-1      LOW-ENERGY PION-PION SCATTERING (New project)

K. Smith (AMD) and J. L. Uretsky . . . . . 35

The s-wave and p-wave amplitudes for low-energy pion-pion scattering have been calculated from the Mandelstam representation for the scattering amplitude. They agree closely with those of Chew, Mandelstam, and Noyes.

- V-50-1      REFLECTION OF A PLANE SOUND WAVE FROM A SINUSOIDAL SURFACE (New project)

J. L. Uretsky . . . . . 35

The reflection coefficients for the various orders of reflection have been calculated for a plane acoustic wave reflected from a two-dimensional, sinusoidal surface on which the pressure vanishes. The general trend of the experimental results agrees with experiment.

- V-52-1      COUPLED-CHANNEL APPROACH TO  $J = \frac{3}{2}^+$  RESONANCES IN THE UNITARY-SYMMETRY MODEL (New project)

A. W. Martin and K. C. Wali . . . . . 40

A dynamical model for baryon-pseudoscalar meson scattering in the  $p_{3/2}$  partial wave has been analyzed in the framework of the Gell-Mann-Ne'eman octet model. Only one unknown parameter enters the calculation, and that



parameter is restricted to a narrow range by comparison with experiment.

PUBLICATIONS . . . . .	43
PERSONNEL CHANGES IN THE ANL PHYSICS DIVISION . . . . .	51

## PROJECTS NOT REPORTED IN THIS ISSUE

A reference to the last preceding report is given in parentheses for each project.

### I. EXPERIMENTAL NUCLEAR PHYSICS

- I-2. Neutron Detectors (ANL-6534, April-May 1962), L. M. Bollinger and G. E. Thomas.
- I-3. Cross-Section Measurements with the Fast Neutron Velocity Selector (ANL-6534, April-May 1962), L. M. Bollinger, R. E. Coté, H. E. Jackson, J. P. Marion, and G. E. Thomas.
- I-7. Gamma-Ray Spectra from Capture in Neutron Resonances (ANL-6603, July-August 1962), H. E. Jackson.
- I-10. Tandem Van de Graaff Accelerator (ANL-6679, January-February 1963), J. R. Wallace.
- I-11. Installation and Operation of the Van de Graaff Generator (ANL-6488, January 1962), J. R. Wallace.
- I-14. Pulsed-Beam Experiments with the Van de Graaff Machine (ANL-6679, January-February 1963), F. J. Lynch and E. N. Shipley.
- I-18. Neutron Polarization and Differential Cross Sections (ANL-6666, November-December 1962), J. E. Monahan and A. J. Elwyn.
- I-19. Nuclear Resonance Absorption of Gamma Rays (ANL-6603, July-August 1962), R. S. Preston, S. S. Hanna, and J. Heberle.
- I-22. Scattering of Charged Particles (ANL-6574, June 1962), H. W. Broek and J. L. Yntema.
- I-24. Studies of Pickup Reactions (ANL-6612, September-October 1962), B. Zeidman and T. H. Braid.
- I-27. Studies of Deuteron-Induced Reactions (ANL-6679, January-February 1963), J. P. Schiffer, L. L. Lee, Jr., and B. Zeidman.

- I-28. Angular Correlations in Charged-Particle Reactions (ANL-6358, April-May 1961), T. H. Braid.
- I-30. Calculation of Reduced Widths from Resonant Scattering of Protons by a Diffuse Potential (ANL-6534, April-May 1962), J. P. Schiffer.
- I-31. Elastic Scattering of Protons (ANL-6679, January-February 1963), L. L. Lee, Jr., and J. P. Schiffer.
- I-35. Decay of  ${}_{57}\text{La}^{135}$  (19.5 hr) (ANL-6391, July-August 1961), S. B. Burson and H. A. Grench.
- I-57. Mu-Mesonic X Rays from Atoms with  $7 \leq Z \leq 30$  (ANL-6679, January-February 1963), C. S. Johnson, H. L. Anderson, E. P. Hincks, S. Raboy, and C. C. Trail.
- I-60. 7.7-Meter Bent-Crystal Spectrometer (ANL-6517, February-March 1962), R. K. Smither.
- I-80. Molecular-Beam Studies (ANL-6612, September-October 1962), W. J. Childs, J. Dalman, D. von Ehrenstein, and L. S. Goodman.
- I-98. Unbound Nuclear Levels in the KeV Region (ANL-6574, June 1962), C. T. Hibdon.
- I-102. Neutron Cross Sections by Self-Detection (ANL-6376, June 1961), J. E. Monahan and F. P. Mooring.
- I-111. Semiconductor Detectors (ANL-6455, November-December 1961), T. H. Braid and J. T. Heinrich.

## II. MASS SPECTROSCOPY

- II-26. Ionization by Ions in the MeV Range (ANL-6679, January-February 1963), S. Wexler and D. C. Hess.
- II-28. Kinetics of Chemical Reactions in the Gas Phase (ANL-6517, February-March 1962), J. Berkowitz and S. Wexler.
- II-29. Gaseous Species in Equilibrium at High Temperatures (ANL-6666, November-December 1962), J. Berkowitz and J. R. Marquart.

- II-39. Fragmentation of Cyanogen (ANL-6488, January 1962), H. E. Stanton.
- II-40. Fragmentation of Hydrocarbons (ANL-6679, January-February 1963), H. E. Stanton and J. E. Monahan.
- II-41. Consecutive Ion-Molecule Reactions (ANL-6603, July-August 1962), S. Wexler.

#### IV. PLASMA PHYSICS

- IV-10. Morphology of High-Frequency Plasmoids (ANL-6574, June 1962), A. J. Hatch.

#### V. THEORETICAL PHYSICS, GENERAL

- V-1. Deformation Energy of a Charged Liquid Drop (ANL-6679, January-February 1963), S. Cohen and W. J. Swiatecki.
- V-2. Properties of Light Nuclei (ANL-6612, September-October 1962), D. Kurath.
- V-3. Dynamics of Nuclear Collective Motion (ANL-6517, February-March 1962), D. R. Inglis.
- V-4. Relative  $\beta$ -Decay Probabilities for  ${}_{19}\text{K}^{40}$  (ANL-6455, November-December 1961), D. Kurath.
- V-8. Relationships of Collective Effects and the Shell Model (ANL-6358, April-May 1961), D. Kurath.
- V-9. Interpretation of Experiments Involving Excitation of the 15.1-MeV Level of  $\text{C}^{12}$  (ANL-6391, July-August 1961), D. Kurath.
- V-11. Resonance Theory of Nuclear Reactions Without Boundary Conditions (ANL-6679, January-February 1963), A. M. Saperstein.
- V-15. Statistical Properties of Nuclear Energy States (ANL-6488, January 1962), N. Rosenzweig.

- V-26. Preacceleration in Electron Theory (ANL-6603, July-August 1962), M. N. Hack.
- V-33. The Supercurrent State (ANL-6679, January-February 1963), M. Peshkin.
- V-38. Particles with Zero Mass and Particles with "Small" Mass (ANL-6679, January-February 1963), F. Coester.
- V-39. Spin and Statistics with an Indefinite Metric (ANL-6603, July-August 1962), R. Spitzer.
- V-42. Time Reversal and Superselection (ANL-6488, January 1962), H. Ekstein.
- V-44. Foundations of Quantum Mechanics (ANL-6679, January-February 1963), H. Ekstein.
- V-45. Meson-Nucleon Interaction (ANL-6666, November-December 1962), L. S. Liu and K. Tanaka.
- V-46. Elastic Nucleon-Nucleon Scattering at High Energies and Small Angles (ANL-6517, February-March 1962), K. Hiida.



I. EXPERIMENTAL NUCLEAR PHYSICS

I-6-1

Double Isomerism in As<sup>73</sup>

(51210-01)

H. H. Bolotin

Odd-A nuclei with an odd neutron or proton number between 29 and 39 are in a region in which many M1 transitions might be expected to show  $\ell$ -forbidden characteristics. In this region, the odd nucleons predominantly occupy the  $p_{3/2}$  and  $f_{5/2}$  orbitals. The configurations of the low-lying states may be complicated and often ambiguous; however, many M1 transitions between levels that are dominantly composed of nucleons in these orbitals would be expected. Such M1 transitions would be  $\ell$  forbidden and would proceed at a retarded rate through admixtures of other configurations in these levels. Retarded M1 transitions have been reported in this region (e. g., in Cu<sup>63</sup>, Ge<sup>73</sup>, As<sup>75</sup>, and Rb<sup>85</sup>), with retardation factors ranging from about 3 to 400 with respect to Moskowsky's single-particle estimates.<sup>1</sup>

The possibility that the 66-keV transition from the first excited state to the ground state in As<sup>73</sup> could be of this retarded type prompted the investigation reported here. The decay of Se<sup>73</sup> has been reported by several groups.<sup>2</sup> The combined work of these investigators shows that the population and decay of the As<sup>73</sup> levels correspond to a simple decay scheme. Only two excited states are populated, with two transitions in cascade and no observed cross-over transition. These transitions have energies of 0.359 and 0.066 MeV and are of M2 and M1

---

<sup>1</sup> A. H. Wapstra, G. J. Nijgh, and R. Van Lieshout, Nuclear Spectroscopy Tables (North-Holland Publishing Company, Amsterdam, 1959), p. 71.

<sup>2</sup> Nuclear Data Sheets, edited by C. L. McGinnis, National Academy of Sciences, National Research Council (U. S. Government Printing Office, Washington, D. C., 1960).

character, respectively.<sup>3, 4</sup> The 0.425-MeV second excited state receives about 99% of the population from the 7.1-hr ground state of  $\text{Se}^{73}$  by means of 70% positron emission and 30% electron capture.<sup>3, 4</sup> Hayward and Hoppes,<sup>4</sup> who have measured the lifetime of the 0.425-MeV second excited state by conventional delayed-coincidence methods, report a half-life of  $6.0 \pm 0.2 \mu\text{sec}$ . These workers also attempted to measure the lifetime of the 0.066-MeV level by the same method and reported an upper limit of  $\leq 5 \text{ nsec}$  for the half-life of this level. The positron spectrum and internal-conversion spectrum of the transitions were investigated by Scott<sup>3</sup> and by Hayward and Hoppes<sup>4</sup> with comparable results. A weak ( $< 1\%$ ) positron branch with an end-point energy 0.36 MeV higher than the main positron group was evidence that the 0.359-MeV transition precedes the 0.066-MeV one.

Scintillation  $\gamma$ -ray spectroscopy was used throughout the work reported here. Delayed-coincidence techniques were used to determine the lifetime of the first excited state and to remeasure that of the second excited state by methods somewhat more refined than those previously used to investigate these levels.

Sources of 7.1-hr  $\text{Se}^{73}$  were produced by the reaction  $\text{Ge}^{70}(\alpha, n)\text{Se}^{73}$  induced by  $\approx 20$ -MeV alpha particles from the Argonne 60-in. cyclotron bombarding targets of naturally occurring elemental Ge. The Ge activity was chemically separated from the target material by standard techniques.

A typical singles pulse-height spectrum recorded with a 3 in.  $\times$  3 in. NaI(Tl) crystal is shown in Fig. 1. The spectrum reveals the presence of only two  $\gamma$  rays (at 66 and 359 keV) in addition to the 511-keV annihilation-radiation peak, in agreement with the results of

---

<sup>3</sup> F. R. Scott, Phys. Rev. 84, 659 (1951).

<sup>4</sup> R. W. Hayward and D. D. Hoppes, Phys. Rev. 101, 93 (1956).

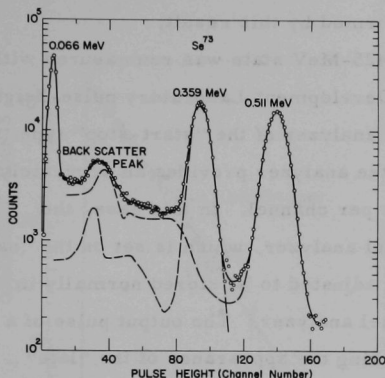


Fig. 1. Singles  $\gamma$ -ray spectrum of the decay of  $\text{Se}^{73}$  as viewed by a 3 in.  $\times$  3 in.  $\text{NaI(Tl)}$  detector. Individual  $\gamma$ -ray contributions are represented by dashed lines.

Hayward and Hoppes. There was no evidence for any other  $\gamma$  rays with energies below 2 MeV.

Delayed-coincidences between the 0.359- and 0.066-MeV gamma rays were studied by use of  $\text{NaI(Tl)}$  detectors and time-to-pulse-height conversion. The  $\gamma$  rays were selected by use of narrow differential pulse-height windows. The results are shown in Fig. 2. The "prompt" response curve was obtained by setting the window on the Compton-electron spectrum of the annihilation quanta from a  $\text{Cu}^{64}$  source. The pulse-height regions were identical to those used in the  $\text{As}^{73}$  cascade. From the slope of the delayed-coincidence spectrum, the 0.066-MeV transition was found to be delayed relative to the 0.359-MeV transition with a half-life of  $(6.1 \pm 0.4) \times 10^{-9}$  sec, which disagrees with the upper limit of  $\leq 5 \times 10^{-9}$  sec reported by Hayward and Hoppes.<sup>4</sup> The time order of the

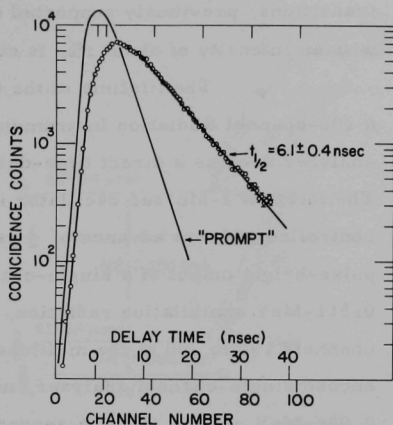


Fig. 2. Time spectrum of coincidences between the 0.066- and 0.359-MeV gamma rays. The delayed slope corresponds to the 0.066-MeV gamma ray being delayed. The prompt spectrum was obtained with a  $\text{Cu}^{64}$  source.

transitions, previously supported only by the observation of a  $\beta^+$  branch<sup>3, 4</sup> with an intensity of about 1%, is confirmed by this result.

The lifetime of the 0.425-MeV state was remeasured with a 200-channel Radiation Instrument Development Laboratory pulse-height analyzer used as a direct time-delay analyzer of the "start-stop" type. The internal 2-Mc/sec oscillator in the analyzer provides an accurately controlled address advance of  $\frac{1}{2}$   $\mu$ sec per channel. In this case, the pulse-height output of a single-channel analyzer, which is set on the "early" 0.511-MeV annihilation radiation, is adjusted to be stored normally in channels 190 to 200 of the multichannel analyzer. The output pulse of a second single-channel analyzer, marking the appearance of the "late" 0.066-MeV gamma ray in a second detector, is delayed by about 15  $\mu$ sec and is used to stop the address-advance oscillator of the multichannel analyzer so that a pulse is artificially stored in a channel corresponding to the time interval between the "early" and "late" pulses. If the "late" pulse does not arrive within about 100  $\mu$ sec after the arrival of the "early" pulse, this pulse is stored in its normal pulse-height channels (190-200). This method of determining a relatively long lifetime in the microsecond region has been used previously.<sup>5</sup> The time spectrum of the 0.511-MeV annihilation radiation and the 0.066-MeV gamma ray is shown in Fig. 3. From the slope of the delay curve, the half-life of the 0.425-MeV level is  $5.0 \pm 0.4$   $\mu$ sec, which differs somewhat from the value  $6.0 \pm 0.2$   $\mu$ sec reported by Hayward and Hoppes who used conventional techniques. The absence of any significant "prompt" portion of this spectrum reflects the fact that positron emission goes almost exclusively to the 0.425-MeV level. Any direct population of the 0.066-MeV state ( $t_{1/2} = 6.1$  nsec) by positron emission would appear as a "prompt" component in Fig. 3.

---

<sup>5</sup> H. H. Bolotin, A. C. Li, and A. Schwarzschild, Phys. Rev. 124, 213 (1961). Detailed specifications for the use of this method are given in this reference. However, footnote 28 of this reference should read "... imposed on pin 7 ..." instead of "... imposed on pin 8 ...".

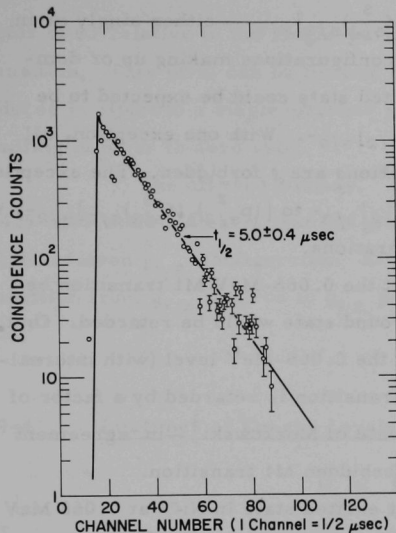


Fig. 3. Time spectrum of coincidences between 0.066-MeV gamma ray and the 0.511-MeV annihilation radiation. The contribution from accidental coincidences has been subtracted.

with other  $\beta$ -decay and internal-conversion work, strongly support the spin and parity assignments given in the decay scheme in Fig. 4. The ground state and first excited state have spin and parity assignments of  $\frac{3}{2}^-$  and  $\frac{5}{2}^-$ , respectively.

As previously mentioned,  $\text{As}^{73}$  is in a region in which the  $p_{3/2}$  and  $f_{5/2}$  orbitals are expected to dominate the configurations of the low-lying levels.  $\text{As}^{73}$  has 33 protons and 40 neutrons. If only the 5 protons in excess of the closed  $f_{7/2}$  shell are considered, the most plausible (but by no means certain or exhaustive) possibilities for the  $\frac{3}{2}^-$  ground state are the configurations  $[(f_{5/2}^4)_0 p_{3/2}]_{3/2}^-$ ,

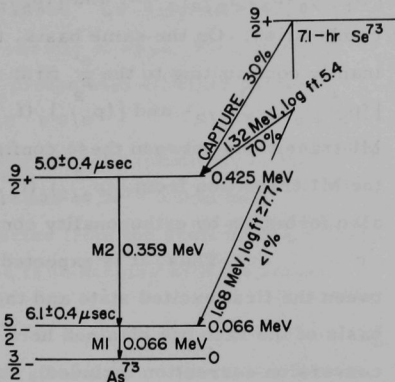


Fig. 4. Decay scheme of the  $\text{Se}^{73}$  ground state, summarizing both previous work and the half-life measurements reported in this paper.

Although the spins of the ground state and excited states of  $\text{As}^{73}$  have not been measured directly, the systematics of levels in this region of atomic weight, together



$[(f_{5/2}^2)_0(p_{3/2}^3)_{3/2}]_{3/2^-}$ , and  $[(p_{3/2}^2)_0(f_{5/2}^3)_{3/2}]_{3/2^-}$ —either singly or in combination. On the same basis, the configurations making up or dominantly contributing to the  $\frac{5^-}{2}$  first excited state could be expected to be  $[(p_{3/2}^4)_0(f_{5/2})_{5/2^-}]$  and  $[(p_{3/2}^2)_0(f_{5/2}^3)_{5/2}]_{5/2^-}$ . With one exception, all M1 transitions between these configurations are  $\ell$  forbidden. The exception, the M1 transition from  $[(p_{3/2}^2)_0(f_{5/2}^3)_{5/2}]_{5/2^-}$  to  $[(p_{3/2}^2)_0(f_{5/2}^3)_{3/2}]_{3/2^-}$ , is also forbidden by orthogonality considerations.

Thus, it is expected that the 0.066-MeV M1 transition between the first excited state and the ground state would be retarded. On the basis of the half-life obtained here for the 0.066-MeV level (with internal-conversion correction included), this transition is retarded by a factor of 97 relative to the single-particle estimate of Moskowsky<sup>1</sup>—in agreement with what would be expected for an  $\ell$ -forbidden M1 transition.

The half-life of the first excited state in  $\text{Ni}^{61}$  at 0.068 MeV has been measured by Holland et al.<sup>6</sup> to be 5.2 nsec. Available evidence<sup>7</sup> indicates that this transition is  $M_1$  in character, going from a  $\frac{5^-}{2}$  first excited state to the  $\frac{3^-}{2}$  ground state in analogy with the 0.066-MeV transition in  $\text{As}^{73}$ . In  $\text{Ni}^{61}$ , there are 33 neutrons which would be expected to form states analogous to those of the 33 protons in  $\text{As}^{73}$ . It is significant, therefore, that the retardation (corrected for internal conversion) in the  $\text{Ni}^{61}$  case is 91—almost identical to that of the 0.066-MeV transition in  $\text{As}^{73}$ .

Both the absence of the crossover transition and the M2 character of the 359-keV transition tend to support the  $\frac{9^+}{2}$  assignment for the 0.425-MeV level. In addition, the 5- $\mu$ sec half-life of this level is in good agreement with its M2 assignment. This transition is retarded by a

---

<sup>6</sup> R. E. Holland, F. J. Lynch, and E. N. Shipley, Bull. Am. Phys. Soc. 5, 424 (1960).

<sup>7</sup> R. H. Nussbaum, A. H. Wapstra, W. A. Bruil, M. J. Sterk, G. J. Nijgh, and N. Grobбен, Phys. Rev. 101, 905 (1956).

factor of 63 relative to the single-particle speed,<sup>1</sup> as is normal for an M2 transition. This level can be formed in a variety of ways, each of which reduces in effect to a single-particle  $g_{9/2}$  proton with all other protons coupling in pairs to zero spin.

The allowed  $\beta$  decay<sup>3, 4</sup> going almost exclusively to the 0.425-MeV state indicates that the ground state of  $\text{Se}^{73}$  would be a single-neutron  $g_{9/2}$  configuration, as expected from the shell model. This transition from  $g_{9/2}$  neutron to  $g_{9/2}$  proton is in keeping with the above data.

I-9-4      Lifetimes of Energy Levels Excited by Slow-Neutron Capture  
(51210-01)

H. H. Bolotin

Despite considerable effort expended by several groups in the study of slow-neutron capture gamma-ray spectra,<sup>1</sup> very few details of many of these spectra are understood. Even for nuclides whose level schemes are on a fairly firm basis, few, if any, parameters (other than energy) describing these levels and the transitions proceeding from them are known.

However, the neutron-capture process is a convenient and direct way of populating a host of low-lying levels, some or all of which may not be reached by other means such as  $\beta$  decay. In many odd-A nuclei, in which several low-lying levels are populated by  $\beta$  decay, the numerous  $\gamma$ -ray decay modes available after neutron capture can often reveal levels and transitions near the ground state which (because of limitations imposed by spin and parity requirements) are inaccessible by  $\beta$  decay. An even greater gap in the availability of levels is found in the case of odd-odd nuclei whose levels, with few exceptions, cannot be reached by

---

<sup>1</sup>G. A. Bartholomew in Nuclear Spectroscopy, edited by Fay Ajzenberg-Selove (Academic Press, Inc., New York and London, 1960), Part A, p. 306.

$\beta$  decay. The levels in odd-odd nuclei are fairly freely populated by processes following slow-neutron capture. In addition, the isotopic identification of these levels is materially facilitated by the fact that most odd-A, even-N targets naturally occur as a single isotope in 100% abundance.

A program has been initiated to investigate low-lying excited states which are populated by slow-neutron capture and subsequent  $\gamma$ -ray decay. The object of this series of investigations is to determine (where feasible) the lifetimes of these levels, and to obtain as much additional information as possible about these levels and the transitions proceeding from them. The lifetimes that fall within the capabilities of the initial circuitry and experimental arrangement are in the range from about 1 - 2 nsec to several microseconds. Only two such experimental studies, both exclusively lifetime determinations, have been reported in the literature.<sup>2, 3</sup>

The experimental work is being carried out at the CP-5 reactor. To provide a beam of thermal and subthermal neutrons free of fast neutrons and pile  $\gamma$  rays, the reactor hole is solidly plugged with lead and bismuth cylinders. The emerging beam then passes through a collimator composed of  $\frac{1}{4}$ -in. Boral sheets and 5-cm lead plates in alternate layers and is incident upon the target mounted at  $45^\circ$  with respect to the beam direction.

Capture  $\gamma$  rays coming from the target are viewed by two scintillation detectors mounted opposite each other at right angles to the beam direction. The scintillators are coupled to 14-stage photomultiplier tubes whose anode signals are limited, clipped, and fed to a 6BN6 time-to-pulse-height converter of the Green and Bell<sup>4</sup> type. Linear signals from

---

<sup>2</sup> N. D'Angelo, Phys. Rev. 117, 510 (1960).

<sup>3</sup> S. J. du Toit and L. M. Bollinger, Phys. Rev. 123, 629 (1961).

<sup>4</sup> R. E. Green and R. E. Bell, Nuclear Instr. and Methods 3, 127 (1958).

an earlier dynode are fed to linear amplifiers and single-channel analyzers and are used to select the events of interest. These pulses are mixed with the output of the time-to-pulse-height converter in a slow triple-coincidence circuit whose output is used to open a linear gate which allows the time spectrum to be displayed on a multichannel pulse-height analyzer.

Since the primary object of these coincidence studies is the measurement of relatively short lifetimes, the time resolution obtainable with plastic scintillators would be highly desirable. Unfortunately, the high complexity inherent in the low-energy portion of the  $\gamma$ -ray spectra resulting from neutron capture requires the highest energy resolution. This requirement demands that at least the low-energy arm of the detector system use NaI(Tl), even at the sacrifice of time resolution. In most cases, the low-lying levels are populated both by high-energy primary  $\gamma$  rays and relatively high-energy  $\gamma$ -ray cascades. Therefore, it is usually sufficient to select a relatively broad portion of the Compton distribution of these high-energy transitions by using a plastic scintillator in the second arm of the coincidence detector system. The use of a plastic scintillator improves the time resolution of the system. With this mixed detector arrangement, half-lives as short as 1 - 2 nsec can be obtained from the slope of the time spectrum, and a lower limit of a few tenths of a nano-second can be set on those half-lives determined from a centroid-shift analysis.

The coincidence circuitry has been fully tested and is performing satisfactorily and the collimator system is almost completed. Relatively severe background problems at the experimental location in the reactor room have necessitated a great deal of care and effort in the selection and arrangement of the detector shielding. Measurements of the type outlined will be undertaken shortly for selected nuclides. In addition, the feasibility of  $\gamma$ - $\gamma$  angular-correlation measurements is being studied.

I-21-11

Excited States of Light Nuclei

(51210-01)

R. G. Allas, S. S. Hanna, L. S. Meyer, and R. E. Segel

RADIATIVE CAPTURE OF PROTONS IN THE  
GIANT RESONANCE

Studies of nuclear reactions initiated by gamma rays have shown that the bulk of the gamma-ray absorption is concentrated in a single resonance which is peaked at a gamma-ray energy of about 20 MeV and has a width of approximately 4 MeV. This giant resonance, which is common to virtually all nuclei, has been the subject of considerable theoretical and experimental attention over the past fifteen years.<sup>1</sup> In many targets the compound nuclei produced by charged particles from the tandem generator are excited to energies corresponding to the giant resonance of gamma-ray absorption. With the highly monoenergetic beams available from the tandem, the  $(p, \gamma)$  reaction can be studied in considerably greater detail than is feasible with the continuous bremsstrahlung spectra used in conventional photonuclear work. Therefore, we have started a program of studying proton-capture gamma rays in the giant resonance region.

The experiments have been set up in the gamma cave at the tandem and use the angular-correlation facility built by T. H. Braid. The gamma-ray detector has been a NaI(Tl) crystal 10 in. in diameter  $\times$  8 in. thick. This crystal, which is one of the largest in use, is mounted on a magnetically shielded photomultiplier tube 12 in. in diameter. The output of the photomultiplier tube is processed by largely conventional electronics. Since pulse pile-up from the intense radiations from  $(p, p')$ ,  $(p, \alpha)$ , and  $(p, n)$  reactions tends to mask the spectrum from the much less numerous but more energetic  $(p, \gamma)$  reactions, a system to strain out pile-up events

---

<sup>1</sup> See for instance, W. E. Stephens in Nuclear Spectroscopy (Academic Press, New York, 1960) and references therein.



has been devised and installed. The final data from the pulse-height analyzer are punched onto IBM cards so that the data can be further processed by the computer. The program subtracts the cosmic-ray spectrum and unpeels the different gamma-ray lines by using a standard line shape of monoenergetic gamma rays (determined for this energy region by an appropriate nuclear reaction at the tandem). The result is a set of intensities of the individual gamma-ray lines.

Several experimental investigations of  $(p, \gamma)$  reactions have been started, including an extensive study of the capture of protons by  $B^{11}$ . For this reaction  $Q=16$  MeV. Thus, since one-twelfth of the proton energy goes into motion of the center of mass, the 12-MeV protons from the tandem excite the compound nucleus to energies up to about 27 MeV. This excitation energy is great enough to permit a complete traversal of the giant resonance, which peaks at an excitation energy of about 22 MeV.

The high-energy end of a typical pulse-height spectrum in the 10 in.  $\times$  8 in. NaI(Tl) crystal when a  $B^{11}$  target is bombarded with protons is shown in Fig. 5. Two distinct and well isolated peaks are shown; they correspond to capture gamma transitions to the ground state and the 4.4-MeV first excited state of  $C^{12}$ . The intensities of these two radiations have been measured both as a function of energy and of angle. The yield curves for these two gamma rays, taken in 25-keV steps at  $90^\circ$  to the incident beam, are shown in Fig. 6. The yield of the ground-state gamma ray shows a resonance shape with the peak of the resonance at a compound-nucleus excitation energy of about 22 MeV, in good agreement with the peak of the gamma-ray absorption curve. Thus the  $(p, \gamma_0)$

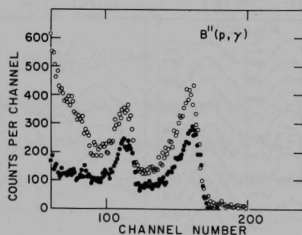


Fig. 5. High-energy end of a typical pulse-height spectrum showing the two capture  $\gamma$  rays from  $B^{11}(p, \gamma_0)C^{12}$  and  $B^{11}(p, \gamma_1)C^{12}$ . The spectrum was recorded with a 10  $\times$  8 in. NaI crystal operated with an anti-pileup circuit.

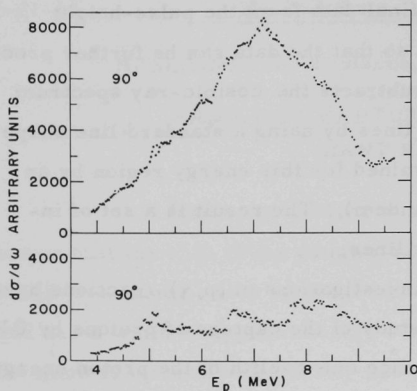


Fig. 6. Yield curves of  $\gamma$  rays from  $B^{11}(p, \gamma_0)C^{12}$  and  $B^{11}(p, \gamma_1)C^{12*}$ , observed at  $90^\circ$  to the proton beam.

the yield for  $\gamma_1$  does not display a simple shape, but rather behaves as if it were primarily due to dissimilar levels in the compound nucleus. This is, of course, what would be expected for  $\gamma_1$ , which should not be in the giant-resonance region.

Angular distributions for  $\gamma_0$  and  $\gamma_1$  were taken in approximately 50-keV steps throughout this region. Some of these are shown in Fig. 7. It can be seen that the  $\gamma_0$  distribution changes smoothly, and

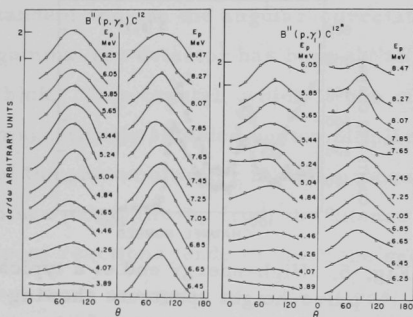


Fig. 7. Angular distributions of  $\gamma$  rays from  $B^{11}(p, \gamma_0)C^{12}$  and  $B^{11}(p, \gamma_1)C^{12*}$ .

reaction shows the same giant resonance as is seen in the inverse gamma-ray-induced reaction. On the other hand, the yield of the first-excited-state gamma ray ( $\gamma_1$ ) does not show the giant-resonance shape and is indeed much smaller throughout the entire region.

When the yield curve  $\gamma_0$  is examined more closely, one sees that it does not have a simple Lorentzian shape but rather exhibits numerous small anomalies. Also,

at the peak of the giant resonance the distribution can be represented approximately by  $1 - \frac{3}{4} \cos^2 \theta$ . The distributions become more isotropic as they are taken at energies farther out on either side of the giant resonance. A slight fore-and-aft asymmetry (i.e., a positive  $\cos \theta$  term) is also present. The structure seen in the yield curve does not seem to greatly disturb the angular dis-

I-50-1

tributions. The  $\gamma_0$  production seems to be chiefly attributable to one state, presumably the giant-resonance state, with some smaller incoherent structure superimposed. On the other hand, the angular distributions for  $\gamma_1$  vary much more and behave as though the  $\gamma_1$  production is primarily due to many levels in the compound nucleus.

Detailed calculations on the giant resonance in  $C^{12}$  have recently been published by Vinh-Mau and Brown.<sup>2</sup> They calculate that the bulk of the giant resonance would be due to a single state formed by promoting a  $1p^{3/2}$  nucleon in  $C^{12}$  to the  $1d^{5/2}$  orbit. This state is calculated to be at 22.2 MeV in the compound nucleus. Our work shows that the proton capture is indeed dominated by a state centered at 22.2 MeV. Furthermore, we can calculate that the angular distribution of the gamma rays for the configuration of Vinh-Mau and Brown would be expected to be  $1 - \frac{3}{4} \cos^2 \theta$ , in good agreement with our measured angular distribution. Thus the theory explains most of the experimental results but makes no allowance for the small structure that appears to be superimposed on the giant resonance.

---

<sup>2</sup> N. Vinh-Mau and G. E. Brown, Nucl. Phys. 29, 89 (1962).

I-50-1      Search for a Particle-Stable Tetra Neutron      (51210-01)

J. P. Schiffer and R. Vandenbosch (CHM)

According to a recent report which has reached us verbally,<sup>1</sup> a study of the  $He^4(\gamma, \pi^+)H^4 \rightarrow T + n$  reaction shows evidence for a narrow ( $\Gamma < 1$  MeV) state in  $H^4$  at about 4 MeV above binding. It is believed to

---

<sup>1</sup> Verbal report at the CERN Conference on High Energy Physics and Nuclear Structure. This experiment with the Frascati synchrotron is a continuation of the one reported by P. E. Argan, C. Bendiscioli, A. Piazzoli, V. Bisi, M. I. Ferrero, and G. Piragino, Phys. Rev. Letters 9, 405 (1962). We are indebted to R. H. Dalitz for calling this work to our attention.

have isotopic spin  $T = 2$ . Starting with this information, using the triton binding energy of 8.48 MeV, and assuming charge symmetry, one would expect the  $n^4$  system to be bound by about 4.5 MeV against particle emission. This nucleus would decay by  $\beta^-$  emission to the  $T = 1$  state of  $H^4$ . This state presumably is the broad anomaly seen in neutron scattering from tritium and it would decay by particle emission.

If the above considerations are valid, the expectation that tetra neutrons should be observed in fission would be highly plausible. Table I lists the number of  $\alpha$ ,  $t$ , and  $p$  particles observed in fission.<sup>2, 3</sup>

TABLE I. Relative frequencies of various real and postulated particles in fission.

Particle	Number observed per $10^5$ fissions	
$\alpha$	500	( $U^{235}$ + thermal $n$ )
$\alpha$	330	( $Cf^{252}$ , spontaneous fission)
$p$	7.4	( $Cf^{252}$ )
$d, He^3$	<1.5	( $Cf^{252}$ )
$t$	20	( $Cf^{252}$ )
$n^4$	<0.002 <0.04	{ from $N^{17}$ activity and the two assumptions stated in the text
$n^4$	<0.0005 (from $Mg^{28}$ activity)	
$n^2$	<0.0005 (from $Mg^{28}$ activity)	

Since the tetra neutron is uncharged, one would expect it to occur at least as often as these particles. From these assumptions it seems reasonable that tetra neutrons should be observed inside nuclear reactors in locations

<sup>2</sup> R. A. Nobles, Phys. Rev. 126, 1508 (1962).

<sup>3</sup> H. E. Wegner, Bull. Am. Phys. Soc. 6, 307 (1961).

where the absorption by nuclei in the moderator is negligible. (There is no reason to assume that the cross section of  $n^4$  on  $C^{12}$  or  $O^{16}$  will be small.) The flux of  $n^4$  might be expected to be at least  $10^{-5}$  of the flux of unmoderated neutrons.

Two experiments have tried to deduce the presence of  $n^4$  by reactions it would produce. In the first experiment,  $N^{14}$  samples were irradiated in the form of three-amino-1,2,4-triazole, whose chemical composition is  $C_2N_4H_3$ . The  $N^{14}(n^4, n)N^{17}$  reaction could have been detected by looking for the 4-sec delayed-neutron activity of  $N^{17}$ . A 3.5-g sample in a pneumatically operated rabbit was irradiated for 5 sec at a point 3 in. from the ends of four fuel elements; and immediately thereafter the sample was counted in a low-background area for a period of 1 min, the number of counts being recorded at 5-sec intervals. Fifty irradiations of  $N^{14}$  samples were interspersed with 50 irradiations of lucite samples of similar weight (chemical composition  $C_8O_2H_{10}$ ). The neutron counter used was borrowed from Dr. G. J. Perlow; it had an estimated over-all efficiency of  $2 \times 10^{-3}$ . Both samples showed a small delayed-neutron activity which could perhaps be attributed to contamination of about  $10^{-9}$  g of natural uranium. In the first minute, the nitrogenous compound gave about 30% more counts than the lucite. The observed difference was  $30 \pm 17$  counts for the first 5 sec,  $6 \pm 12$  counts for the second 5 sec, and  $63 \pm 20$  counts for the remaining 50 sec. If the cross section for the absorption of  $n^4$  by D and  $O^{16}$  in the moderator is assumed to be 0.5 barns, the mean free path in the moderator is 25 cm. Furthermore, if the cross section of the  $N^{14}(n^4, n)N^{17}$  reaction is assumed to be 50 mb, a value that seems reasonable from  $(\alpha, p)$  and  $(\alpha, n)$  cross sections on light nuclei, these numbers yield the result that the number of tetra neutrons per fission is less than  $2 \times 10^{-8}$ . On the assumption that the interaction cross section with the moderator nuclei is 1 b and the cross section for producing  $N^{17}$  is 10 mb, this number becomes  $4 \times 10^{-7}$ .

In the second experiment, we looked for  $\text{Mg}^{28}$  produced by the  $\text{Al}^{27}(\text{n}^4, \text{H}^3)\text{Mg}^{28}$  or  $\text{Al}^{27}(\text{n}^4, \text{p}2\text{n})\text{Mg}^{28}$  reaction. The  $\text{Mg}^{28}$  has the advantage of having a reasonably long half-life (21 hr) and also of being far enough away from stable isotopes so that it cannot easily be produced by neutron capture by contaminants in the target material. A 1.4-g sample of very pure Al was irradiated for 24 hr in a vertical thimble in the center of the central fuel element of CP-5. A radiochemical separation of Mg was then performed. The Mg sample was counted with a  $3 \times 3$ -in. NaI(Tl) scintillation counter and the resulting spectrum was examined for evidence of the 1.35-MeV gamma from the decay of  $\text{Mg}^{28}$  and the 1.78-MeV gamma from the  $\text{Al}^{28}$  which would be in radioactive equilibrium with  $\text{Mg}^{28}$ . A slight increase was observed at 1.35 MeV but no increase above background was found at 1.75 MeV. On the assumption that only tetra neutrons from the fuel element used can contribute and that the cross section for producing  $\text{Mg}^{28}$  is 40 mb, we conclude that the number of tetra neutrons per fission is less than  $5 \times 10^{-9}$ .

Table I summarizes our results together with known probabilities for emitting other particles in fission.

These results may also be used to set a limit on the number of particle-stable di neutrons emitted in fission. In the first measurement one might perhaps expect some activity from the  $\text{O}^{18}(\text{n}^2, \text{p})\text{N}^{17}$  reaction from the  $\text{O}^{18}$  in the lucite sample. However, the Q-value for this is -4 MeV and therefore it is not a very satisfactory test. In the second experiment the  $\text{Al}^{27}(\text{n}^2, \text{p})\text{Mg}^{28}$  reaction has a positive Q-value and therefore should be observed. The lack of  $\text{Mg}^{28}$  activity can be interpreted as showing that the number of di neutrons in fission has the same limit as the one set for tetra neutrons from this activity. This limit seems to be several orders of magnitude below the value set by earlier experiments<sup>4</sup>

---

<sup>4</sup> F. W. Fenning and F. R. Holt, *Nature* 165, 722 (1950); A. J. Ferguson and J. H. Montague, *Phys. Rev.* 87, 215 (1952).

attempting to detect di neutrons in fission, mostly because these looked for activities induced by di neutron capture (for which the cross sections would be considerably lower) and the measurements were done in reactors with lower neutron fluxes.

I-55-13      Capture Gamma-Ray Spectra for Neutrons with Energies  
from 0.1 to 10 eV      (51210-01)

S. Raboy and C. C. Trail

GAMMA RADIATION FROM NEUTRON  
CAPTURE BY DEUTERIUM

Earlier attempts to measure the capture cross section of deuterium were based on tritium production<sup>1</sup> or the diffusion of a neutron beam in heavy water.<sup>2</sup> Since the cross section is about 0.5 mb, the direct observation of the capture gamma ray has been limited to capture of neutrons by the heavy water serving as moderator in a reactor.<sup>3</sup>

At the Argonne research reactor CP-5, we have a clean neutron beam from a cobalt mirror,<sup>4</sup> a scintillation spectrometer<sup>5</sup> which yields gamma-ray spectra of good quality, and a shield which keeps the background in the spectrometer quite small. This apparatus enables one to view the capture gamma ray from deuterium directly. We report a measurement of the capture cross section relative to that for the proton. The measurement of the energy of the emitted gamma ray is in progress.

---

<sup>1</sup> Louis Kaplan, G. R. Ringo, and K. E. Wilzbach, Phys. Rev. 87, 785 (1952).

<sup>2</sup> B. W. Sargent, D. V. Booker, P. E. Cavanagh, H. G. Hereward, and N. J. Neimi, Can. J. Research 25A, 134 (1947).

<sup>3</sup> B. B. Kinsey and G. A. Bartholomew, Phys. Rev. 80, 918 (1950).

<sup>4</sup> M. T. Burgy, V. E. Krohn, T. B. Novey, G. R. Ringo, and V. Telegdi, Phys. Rev. 110, 1214 (1958).

<sup>5</sup> C. C. Trail and S. Raboy, Rev. Sci. Instr. 30, 425 (1959).



The neutron beam from the reactor is reflected by a cobalt mirror<sup>4</sup> and enters the shielding around the scintillation spectrometer. The average energy of the neutron beam is about 0.01 eV as measured by transmission through gold.

The capture gamma rays emitted by the sample irradiated by this neutron beam are observed with two scintillation spectrometers. Each spectrometer consists of a central crystal 2.5 in. in diameter and 6 in. long coupled to a photomultiplier. The pulses from each of these counters are analyzed in one half of a 512-channel analyzer. Two sets of data were obtained in which the pulses from one counter were analyzed by all 512 channels.

Around each central crystal is an annulus of NaI, 8 in. in diameter and 12 in. long. Each annulus is viewed by six photomultipliers whose anodes are connected in parallel. If degraded radiation escapes the center crystal and loses as much as about 30 keV in the annulus, the event is discarded electronically. In this way the Compton distribution and escape peaks associated with pair creation are suppressed.

The shielding around the counters weighs 13 tons; it is designed to protect the crystals from neutrons and gamma rays in the room.

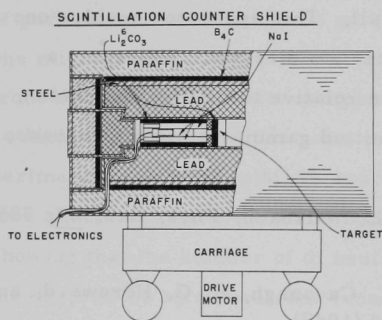


Fig. 8. A cutaway view of the shield, showing one scintillation spectrometer. The neutron beam is incident normal to the plane of the figure.

A cutaway view of the shield and one spectrometer is shown in Fig. 8. A slot 2 in. wide and 7 in. high permits the beam to pass through the shield. Except near the aperture of the counters, the slot is lined with  $\frac{1}{4}$  in. of Boral to capture scattered neutrons. The target is positioned in an aluminum holder in the center of the shield. Between the target and each counter is a shield of lithium carbonate (1 in.

thick) enriched to 95%  $\text{Li}^6$  and a lead collimator 2 in. thick with a hole 1.5 in. in diameter. The lithium carbonate is contained in a Teflon shell with a wall thickness of about  $\frac{1}{16}$  in. Around each annulus is a 1-in. layer of enriched lithium carbonate in an iron shell. These shields are enveloped in three more concentric cylinders: 9 in. of lead, 1 in. of  $\text{B}_4\text{C}$ , and 6 in. of paraffin. For structural reasons, an iron shell 10 in. in diameter and 1 in. thick forms the inner cavity which contains the counters and lithium carbonate. The entire shield is mounted on wheels so that it can be used with a neutron monochromator.

The capturing sample consisted of  $120.7 \pm 0.1$  ml of  $\text{D}_2\text{O}$  to which was added  $4.20 \pm 0.10$  ml of  $\text{H}_2\text{O}$ . The sample was contained in a Teflon cylinder 1.75 in. in diameter and 4 in. high. The container wall was about  $\frac{1}{16}$  in. thick and the sample was held in place by an aluminum wire which was outside the aperture of the spectrometer.

The gamma-ray spectrum from one counter is shown in Fig. 9. The peaks at 2.2 and 6.2 MeV are emitted as a result of capture of neutrons by hydrogen and deuterium, respectively. The peak at 6.8 MeV is attributed to capture of neutrons in the NaI crystals and the peak at 7.6 MeV is from capture by iron in the surroundings. The gamma rays from iron and light water provide the energy calibration of the abscissa. The small hump on the low-energy side of the deuteron-capture line is attributed to a

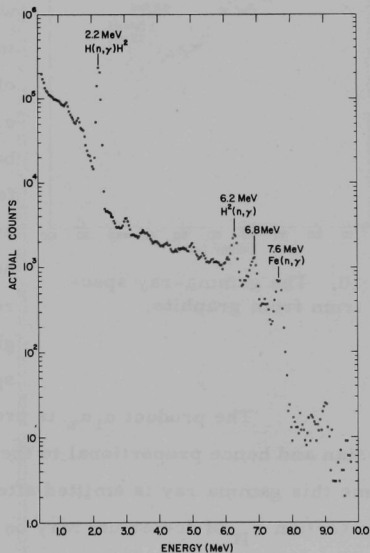


Fig. 9. The gamma-ray spectrum from heavy water. These data were collected in about 18 hr.

6-MeV transition in Fe. The backgrounds are obtained by replacing the water with a graphite sample and normalizing the spectra to the 6.8- and 7.6-MeV peaks. A typical spectrum from graphite is shown in Fig. 10.

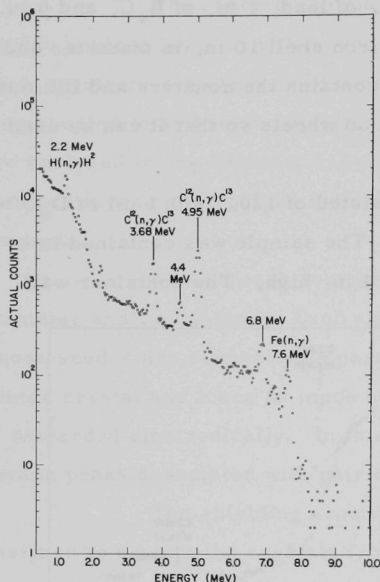


Fig. 10. The gamma-ray spectrum from graphite.

By means of a chi-squared minimization method,<sup>6</sup> the photopeaks associated with the gamma rays are fitted to a Gaussian of the form

$$y(x_j) = a_1 \exp \left( \frac{a_2 - x_j}{a_3} \right)^2 + a_4, \quad (1)$$

where  $y(x_j)$  is the number of counts in channel  $x_j$ ,  $a_1$  is the peak amplitude of the Gaussian,  $a_2$  its peak position,  $a_3$  its width, and  $a_4$  any residual background. An error is computed for each parameter and the errors are normalized for any differences between the  $\chi^2$  of the fit and the  $\chi^2$  reported for the calculation. Table II gives a set of results for a typical spectrum.

The product  $a_1 a_3$  is proportional to the area of the Gaussian and hence proportional to the yield of the gamma ray. If we assume this gamma ray is emitted after each neutron capture, the capture cross section  $\sigma_D$  of deuterium may be calculated from the relation

<sup>6</sup> R. Julke, J. E. Monahan, S. Raboy, and C. C. Trail, Argonne National Laboratory Topical Report ANL-6499 (unpublished).

TABLE II. Parameters for the Gaussian in Eq. (2). These were obtained with a chi-squared minimization calculation.

Gamma-ray energy (MeV)	$a_1$ (counts)	$a_2$ (channel)	$a_3$ (channel)	$a_4$ (counts)	$\chi^2$	
					Calc.	Expected
2.2	$(2.213 \pm 0.006) \times 10^5$	$58.018 \pm 0.003$	$1.780 \pm 0.004$	$187 \pm 167$	5.8	3
6.2	$1820 \pm 53$	$164.50 \pm 0.10$	$3.20 \pm 0.18$	$-130 \pm 52$	0.9	3

$$\sigma_D = \sigma_H \left[ \frac{(a_1 a_3)_D}{(a_1 a_3)_H} \cdot \frac{N_H}{N_D} \cdot \frac{(PE)_H}{(PE)_D} \cdot \frac{T_H}{T_D} \right], \quad (2)$$

where the subscripts D and H refer to deuterium and hydrogen,  $a_1$  and  $a_3$  are as defined above,  $N$  is the number of atoms in the sample,  $PE$  is the photoefficiency of the crystal, and  $T$  is the transmission of the gamma ray through the 1-in. thickness of the lithium carbonate shield and one half the thickness of the water sample. We calculate<sup>7</sup> that  $T_H/T_D = 0.92$  and estimate an uncertainty of 0.03. The photoefficiencies are calculated by a Monte Carlo method.<sup>8</sup> The ratio  $(PE)_H/(PE)_D$  is calculated to be  $2.26 \pm 0.11$ , the uncertainty arising from the statistical uncertainty of the Monte Carlo calculation and the possible systematic uncertainties of the calculation. The ratio  $N_H/N_D$  is  $3.866 \times 10^{-2}$ .

Table III summarizes the ratios of the areas for six measure-

TABLE III. Ratio of the areas of the capture gamma rays from hydrogen and deuterium.

Run No.	$\frac{(a_1 a_3)_D}{(a_1 a_3)_H}$
358	$(1.48 \pm 0.19) \times 10^{-2}$
364	$(1.47 \pm 0.11) \times 10^{-2}$
380	$(1.34 \pm 0.08) \times 10^{-2}$
381	$(1.28 \pm 0.08) \times 10^{-2}$
382	$(1.48 \pm 0.16) \times 10^{-2}$
383	$(1.29 \pm 0.12) \times 10^{-2}$
Weighted average	$(1.35 \pm 0.04) \times 10^{-2}$

<sup>7</sup> Gladys White Grodstein, U. S. National Bureau of Standards Circular 583.

<sup>8</sup> W. F. Miller and W. J. Snow, Rev. Sci. Instr. 31, 39 (1960), and private communication.

ments. A weighted average of these results gives  $(a_1 a_3)_D / (a_1 a_3)_H = (1.35 \pm 0.4) \times 10^{-2}$ . We then use Eq. (2) to combine this result with the other parameters mentioned above. The result is  $\sigma_D / \sigma_H = (10.9 \pm 0.8) \times 10^{-4}$ . If we assume that  $\sigma_H = 332 \pm 2$  mb,<sup>9</sup> then  $\sigma_D = 0.362 \pm 0.026$  mb. Previous measurements have reported  $0.46 \pm 0.11$  mb<sup>1</sup> and  $0.57 \pm 0.01$  mb.

A measurement of the energy of the transition is in progress.

---

<sup>9</sup> S. P. Harris, C. O. Muehlhause, D. Rose, H. P. Schroeder, G. E. Thomas, Jr., and S. Wexler, Phys. Rev. 91, 125 (1953).





## II. MASS SPECTROSCOPY

II-23-2     Sputtering Experiments in the Rutherford Collision Region  
(51300-01)

M. Kaminsky

ATOMIC COLLISION SEQUENCES IN THE LATTICES OF METAL  
MONOCRYSTALS BOMBARDED WITH IONS IN THE  
RUTHERFORD COLLISION REGION

In the experiments described, the (100) planes of copper monocrystals were bombarded with deuterons. The angles of incidence ranged from  $0^\circ$  to  $45^\circ$  from the normal and the energies from 0.10 to 0.25 MeV (from Cockroft-Walton generators) and from 0.70 to 2.0 MeV (from a Van de Graaff). In this energy range the energy of an incident ion is high enough that the collision can be treated in terms of the Coulomb repulsion between the nuclei (Rutherford collision). The particles back sputtered from the target were collected on a quartz cylinder surrounding the target. Details of the experimental arrangement have been reported earlier.<sup>1,2</sup>

It has been possible to establish the existence of preferred ejection directions in the back sputtering<sup>3</sup> of target particles for the Rutherford collision region, despite the fact that the mean free path of the incident particle is of the order of several thousand angstroms. In contrast to the cosine distribution to be expected if the mechanism were evaporation of target material from a hot spot or a heated spike along the path of the incident ion, as predicted by some theoretical treatments, a

---

<sup>1</sup> M. Kaminsky, Phys. Rev. 126, 1267 (1962).

<sup>2</sup> M. Kaminsky, Physics Division Summary Report ANL-6488 (January 1962), p. 3.

<sup>3</sup> In back sputtering, the target particles leave from the surface which is struck by the incident ion beam, while in forward sputtering they leave from the opposite surface [M. W. Thompson, Phil. Mag. 4, 139 (1959)]. In the latter case, however, the ratio of the target thickness to the range of the incident particles becomes an important parameter in the target-particle ejection in transmission.

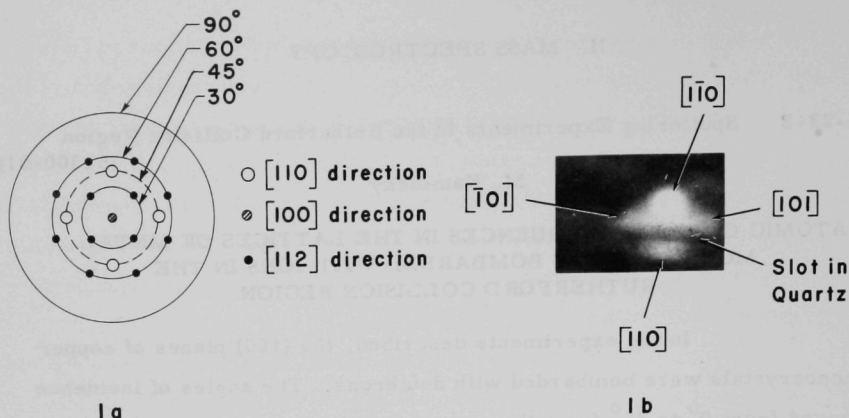


Fig. 11 (a) Stereographic projection of a face-centered-cubic lattice onto a plane parallel to a (100) lattice plane. The figure shows only the  $[110]$ ,  $[100]$ , and  $[112]$  directions. Those coinciding with the  $90^\circ$  circle are omitted. (b) Autoradiogram showing the pattern of preferential ejection directions when a Cu(100) surface is bombarded with 125-keV deuterons incident at  $31^\circ$ . Most of the deposit is in the four  $[110]$  spots, the  $[110]$  spot being the densest, while the  $[11\bar{0}]$  spot is partially hidden by the slot in the quartz.

distinct spot pattern is observed (Fig. 11). The four main spots, corresponding to the  $[110]$  directions, were conspicuous at all the angles of incidence. Additional spots corresponding to the  $[112]$  and  $[100]$  crystal directions were also observed throughout the investigated range of angles of incidence, but their densities were smaller than those corresponding to the  $[110]$  directions. With increasing angle of incidence, the deposits corresponding to the  $[112]$  and  $[100]$  directions became less dense. Optical transmission measurements of the deposits revealed that for ions incident at  $45^\circ$  approximately 75% of the sputtered material is in the four main spots ( $[110]$ ,  $[1\bar{1}0]$ ,  $[101]$ , and  $[1\bar{0}1]$  spots) and about 60% for ions incident at  $25^\circ$ .

Another significant observation was the increasing asymmetry in the densities of the four spots as the angle of incidence  $\alpha$  increased. This seems to indicate an anisotropy in the momentum distribution of the

primary recoil atoms, in contradiction to recent predictions of Nelson and Thompson.<sup>4</sup> For instance, as the direction of incidence approaches the  $[110]$  direction ( $\theta \rightarrow 45^\circ$ ), the density of the spot corresponding to the  $[\bar{1}\bar{1}0]$  direction increases relative to the densities of the  $[101]$  and  $[\bar{1}01]$  spots, as shown in Fig. 11 (b) for  $\theta = 31^\circ$ . At  $\theta = 45^\circ$ , the density of the  $[\bar{1}\bar{1}0]$  spot is about 1.8 times that of the other two. The method used here seems to offer a new tool to study the momentum distribution of primary recoil atoms.

The sputtering ratio (sputtered particles per incident ion) depends strongly and in a complicated way on the angle of incidence. Instead of increasing monotonically with increasing  $\theta$ , it drops at certain angles. For example, near  $\theta = 45^\circ$  it drops to about the value at  $0^\circ$  but the intensities in the deposits of corresponding spots are different for the two angles. Optical transmission measurements (Fig. 12) show that the

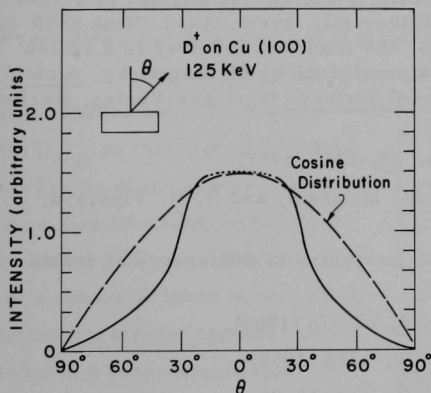


Fig. 12. Density distribution in an individual  $[110]$  spot. The deposit of particles was sputtered from a  $\text{Cu}(100)$  plane by bombardment with 125-keV  $\text{D}^+$  ions under normal incidence.

distribution in an individual spot is Gaussian, not cosine, and nearly independent of the angle of incidence. This result indicates that the recently suggested mechanism of sputtering by heated spikes<sup>5</sup> is of no major importance in these experiments.

The experiment clearly establishes the existence of preferred ejection directions in "back sputtering" for the Rutherford collision region, in which the sputtered particles are ejected from the surface struck by the incident ions. This result is surprising

<sup>4</sup>R. S. Nelson and M. W. Thompson, Proc. Roy. Soc. A259, 458 (1961), particularly p. 468.

<sup>5</sup>M. W. Thompson and R. S. Nelson, Phil. Mag. 7, 2015 (1962).

since the incident particle has a mean free path  $\lambda$  of several thousand angstroms in the target crystal (e.g., for 500-keV  $D^+$  on Cu,  $\lambda \approx 8000 \text{ \AA}$ ), so that the displaced target atoms must undergo many collisions before they escape from the lattice. All previous experiments on the preferred directions of back sputtering<sup>6</sup> have been in the hard-sphere collision region; and the mean free paths of the incident ions have been 2 - 3 orders of magnitude smaller than in the present experiment. Because of these short ranges, the observed ejection patterns are not properly applicable as tests of the extended focused collision sequences postulated in the models of Silsbee,<sup>7</sup> Gibson et al.,<sup>8</sup> Thompson et al.,<sup>4,5,9,10</sup> Leibfried et al.,<sup>11-14</sup> and Oen et al.<sup>15</sup>

---

<sup>6</sup> G. S. Anderson and G. K. Wehner, J. Appl. Phys. 31, 2305 (1960); M. Koedam and A. Hoogendorn, Physica (den Haag) 26, 351 (1960); M. W. Thompson and R. S. Nelson, AERE-R 3320 (1960); R. S. Nelson and M. W. Thompson, Phil. Mag. 7, 1425 (1962), Phys. Letters 2, 3, 124 (1962); V. A. Molchanov, V. G. Telkovskii, Izvest. Akad. Nauk SSSR 26, 1359 (1962). For more references, the reader is referred to a review article on sputtering contained in a monograph by M. Kaminsky, Atomic and Ionic Impact Phenomena on Metal Surfaces (Springer-Verlag, Berlin, in press).

<sup>7</sup> R. H. Silsbee, J. Appl. Phys. 28, 1246 (1957).

<sup>8</sup> J. B. Gibson, A. N. Goland, M. Milgram, and G. H. Vineyard, Phys. Rev. 120, 1229 (1960).

<sup>9</sup> M. W. Thompson, Proc. Fifth International Conference on Ionization of Gases, Munich, 1961.

<sup>10</sup> M. W. Thompson, Phil. Mag. 5, 51 278 (1960).

<sup>11</sup> G. Leibfried, J. Appl. Phys. 30, 1388 (1959).

<sup>12</sup> G. Leibfried, J. Appl. Phys. 31, 117 (1960).

<sup>13</sup> Chr. Lehman and G. Leibfried, Z. Physik 162, 203 (1961).

<sup>14</sup> P. H. Dederichs and G. Leibfried, Z. Physik 170, 320 (1962).

<sup>15</sup> O. S. Oen, D. K. Holmes, and M. T. Robinson, J. Appl. Phys. 34, 302 (1963).

In such a model as applied to the Rutherford collision region, the incident particle undergoes Coulomb collisions with the nuclei of the target atoms along its path and displaces them from their lattice sites as "primary knock-ons." If the mean energy of the primary knock-ons exceeds the displacement energy of a lattice atom (about 25 eV for Cu, about 21 eV for Ag), then they in turn suffer hard-sphere collisions with neighboring lattice atoms and produce secondary displacements. Such successive collisions continue until the energies of the displaced atoms fall to about the displacement energy. Some of these displaced atoms may reach the surface and escape. The accepted belief has been that lattice particles displaced by Rutherford collisions would undergo so many collisions before leaving the surface that they would leave in random directions, contrary to the result reported here. However, Silsbee<sup>7</sup> has pointed out that in a monocrystal regarded as rows of equal hard spheres, momentum may be focused along a line of atoms in a close-packed crystal direction.

Figure 13 shows schematically such a line of hard and equal spheres along the x axis, with  $D_{hkl}$  as the spacing between the centers of the spheres along such a line (the subscripts h, k,  $\ell$  are Miller indices). The diameter  $d$  of a sphere is taken equal to the distance of closest approach of the atoms in a head-on collision. If two spheres collide at the collision point P, the knocked-on second sphere moves in the direction PC

making an angle  $\theta_1$  with the x axis since momentum is transferred only in the direction of the radius vector between the centers of the two spheres. The incident atom bounces off perpendicular to the direction PC. For

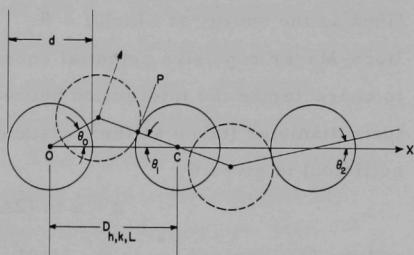


Fig. 13. Schematic illustration of Silsbee's mechanism for the propagation of an energy pulse along a close-packed line of hard spheres.

small values of the angle  $\theta_0$  between the x axis and the momentum of the incident atom, the relation between  $\theta_1$  and  $\theta_0$  can be shown to be

$$\theta_1 = \theta_0 \left( \frac{D_{hkl}}{d} - 1 \right). \quad (1)$$

Silsbee focusing occurs whenever  $f = \theta_{n+1} / \theta_n < 1$  or, in other words, whenever  $D_{hkl} / d < 2$ ; the successive angles become monotonically smaller. The final result is a sequence of head-on collisions without any change of angle, and energy losses along the chain may be neglected. In this case the collisions do not displace the lattice atoms from their original equilibrium positions and no mass transport occurs.

In the case of the Cu monocrystal in the present investigation, Silsbee's focusing condition  $f < 1$  is fulfilled only for the most densely-packed crystal directions of such a face-centered cubic crystal, the [110] directions. These are in fact the crystal directions in which the present experiment shows the strongest sputtering effect (Fig. 11). A focusing energy  $E_f$ , below which Silsbee focusing occurs, can be defined as the energy at which  $f = \theta_{n+1} / \theta_n = 1$  and  $D_{hkl} / d = 2$ . If a Born-Mayer repulsive potential energy  $E_\phi = A \exp(-a/r)$  is assumed to characterize the interaction between two ion cores in the lattice, then their diameter (taken as their distance of closest approach in a head-on collision) is given by

$$d = a \ln(2A/E) \quad (2)$$

and the focusing energy in the [110] direction is

$$E_f^{110} = 2A \exp(-D_{110}/2a). \quad (3)$$

Thompson,<sup>7</sup> using  $A = 20$  keV and  $a = D/13$  from data for the compressibility of copper,<sup>16</sup> obtained  $E_f = 60$  eV, while the machine calculations of Vineyard et al.<sup>8</sup> led to only  $E_f = 30$  eV.

<sup>16</sup>

H. B. Huntington, Phys. Rev. 93, 1414 (1954).

Leibfried,<sup>11</sup> Thompson,<sup>7</sup> and Gibson *et al.*<sup>8</sup> showed that the energy attenuation in such focused collision sequences is due to interaction with atoms in adjacent close-packed lines. By moving along a  $[110]$  direction in a fcc crystal, the atom shortens the distance between itself and four atoms (denoted in Fig. 14 as  $B_1$ ,  $B_2$ ,  $B_3$ , and  $B_4$ ) in neighboring lines. The resulting increase in the repulsive potential leads to an energy loss for which reported values vary between  $\frac{2}{3}$  and 1 eV per collision.<sup>8,4</sup>

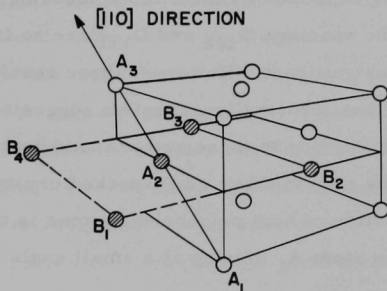


Fig. 14. Schematic illustration of a hard-sphere collision chain along the  $[110]$  direction in a fcc crystal.

On the basis of their estimates of the focusing energy and the energy loss per collision, Nelson and Thompson<sup>4</sup> calculated that the range  $r$  of such focused collision sequences in the  $[110]$  direction is about  $206 \text{ \AA}$ . This estimate of  $r$  seems too low since most of the more energetic primary knock-ons in the present experiment (and also the less energetic secondary knock-ons which eventually lead to atomic collision sequences) are produced several thousand angstroms below the surface. This becomes even more convincing if one considers that in the investigated range of ion energies the secondary knock-ons are more numerous than the primaries. For instance, for the case of 500-keV deuterons incident on copper the average number  $\bar{\nu}$  of secondary knock-ons per primary knock-on is about 4.3, as can be calculated on the basis of an expression given by Seitz and Koehler.<sup>17</sup> (The latter result is indicated by the absolute values of the sputtering ratio and its energy dependence in this energy range.<sup>1</sup>) The results would also be changed substantially if other constants were used

<sup>17</sup> F. Seitz and J. Koehler, *Solid State Physics*, edited by F. Seitz and D. Turnbull (Academic Press, Inc., New York, 1956), Vol. 2, p. 307.





[100] direction may be treated as a converging lens with a focal length given (for small values of  $\theta_0$ ) by  $f_{hkl} \approx \frac{1}{2} a_0 (\theta_0 / \psi)$ , where  $a_0$  is the lattice constant<sup>4</sup> and  $\psi = \theta_1 - \theta_1'$ . This "lens focusing" mechanism is energetically less efficient than Silsbee's hard-sphere focusing and would be expected to become important only at higher energies. Using an iterative computing method, Vineyard et al.<sup>2</sup> found that in a fcc lattice the effectiveness of atomic collision sequences decreases in the order [110], [111], [100], a result which is in qualitative agreement with our experimental observation.

A forthcoming report will describe similar results for a (100) plane of a silver monocrystal. Other investigations that have been conducted include mass spectrometric investigations of the species of sputtered target particles, electron microscopic studies of the ionic etching effect of high-energy ions on metal monocrystalline surfaces, and the dependence of the sputtering ratio on the energy and the type of the incident ion for the Rutherford collision region.



V. THEORETICAL PHYSICS, GENERAL

V-49-1.                      Low-Energy Pion-Pion Scattering                      (51151-01)

Kenneth Smith (AMD) and Jack L. Uretsky

This calculation starts with the partial-wave dispersion relations for pion-pion scattering as deduced from the Mandelstam representation for the scattering amplitude. The contribution of the "left-hand cut" was calculated from  $\lambda\phi^4$  perturbation theory (to second order in  $\lambda$ ). The s-wave and p-wave amplitudes were obtained numerically and found to agree closely with those obtained by Chew, Mandelstam, and Noyes who proceeded from a different viewpoint.

A report on this work has been prepared for publication.

V-50-1.                      Reflection of a Plane Sound Wave from a Sinusoidal Surface\*                      (51300-01)

Jack L. Uretsky

We consider the problem of a plane acoustic wave reflected from a two-dimensional, sinusoidally shaped surface on which the pressure vanishes.<sup>1</sup> The following paragraphs contain a brief description of the technique of solution, and the accompanying figures compare the results with the experiment of La Casce and Tamarkin.<sup>2</sup> A more complete discussion of this marvelously complex problem is in preparation.

---

\* A considerable part of this work was done at the Marine Physical Laboratory of the Scripps Institute of Oceanography, University of California, San Diego.

<sup>1</sup> This problem was stated, and incorrectly treated, by Lord Rayleigh, Theory of Sound (Dover Publications, Inc., New York, 1945), Sec. 272a. A good bibliography of subsequent work prior to 1958 is contained in the review article by Iu. P. Lysanov, Soviet Phys. Acoustics 4, 1 (1958).

<sup>2</sup> E. O. La Casce, Jr., and P. Tamarkin, J. Appl. Phys. 27, 138 (1956).

Formally, we are concerned with the solution of the integral equation obtained from<sup>3</sup>

$$\psi(x, y) = \psi_1(x, y) + \frac{1}{4}i \int_{-\infty}^{\infty} dx' H_0(k|\underline{r} - \underline{r}'|) \phi(x') \quad (1)$$

by putting the  $y$  coordinate on the bounding surface where the left-hand side vanishes. The quantity  $H_0(x)$  is the usual Hankel function of the first kind. The bounding surface is

$$y = \eta(x) = b \cos p x, \quad (2)$$

and  $\underline{r}'$  refers to an arbitrary point on the surface with coordinates  $[x', \eta(x')]$ . The quantity  $\phi(x')$  is related to the normal derivative of the velocity potential  $\psi(x, y)$  evaluated at the reflecting surface, and the incident wave is given by

$$\psi_1(x, y) = \exp i k [\lambda_0 x - \mu_0 y]. \quad (3)$$

This defines the notation for the wave number  $k$  and the direction cosines  $\lambda_0$  and  $\mu_0$ .

The crucial step in the present formulation of the problem is to recognize that  $\phi(x)$  admits of a Fourier series representation

$$\phi(x) = k \sum_{j=-\infty}^{\infty} i^{-j} A_j \exp[ik(\lambda + jp/k)x] \equiv k \sum_j i^{-j} A_j \exp(ik\lambda_j x), \quad (4)$$

so that the integral equation obtained from Eq. (1) can be transformed into an infinite set of linear equations

$$\sum_{j=-\infty}^{\infty} M_{nj} A_j = (-1)^n J_n(bk\mu_0). \quad (5)$$

---

<sup>3</sup>P. M. Morse and H. Feshbach, Methods of Theoretical Physics (McGraw-Hill Book Co., Inc., New York, 1953), pp. 811 ff.

The (complex) matrix elements  $M_{nj}$  are given by

$$M_{nj} = -(2\pi)^{-1} \sum_{\ell=-\infty}^{\infty} (-1)^{\ell} \int_{-\infty}^{\infty} dt (t^2 - \mu_{\ell}^2)^{-1} J_{n-\ell}(bkt) J_{\ell-j}(bkt), \quad (6)$$

where the  $J_{\ell}(x)$  are the usual Bessel functions and  $\mu_{\ell}$  is the sine of the grazing angle of the  $\ell$ -th-order reflection coefficient and is given by

$$\mu_{\ell} = (1 - \lambda_{\ell}^2)^{1/2} = +i(\lambda_{\ell}^2 - 1)^{1/2}. \quad (7)$$

The  $\lambda_{\ell}$  were defined in Eq. (4).

Finally, the physically interesting quantities (the reflection coefficients for the various orders of reflection) are determined from the boundary coefficients  $A_j$  by use of the relation

$$R_{\ell} = (2\mu_{\ell})^{-1} \sum_{j=-\infty}^{\infty} A_j J_{\ell-j}(bk\mu_{\ell}). \quad (8)$$

The major complication of the problem (other than the usual difficulties associated with inverting infinite matrices) is in the calculation of the matrix elements  $M_{nj}$ . For fixed  $\ell$  in the summation of Eq. (6), the integral may be shown to be

$$-i(2\mu_{\ell})^{-1} J_{n-\ell}(bk\mu_{\ell}) J_{\ell-j}(bk\mu_{\ell}) + (bk) R_{n,j}^{\ell}(bk\mu_{\ell}). \quad (9)$$

The function  $R_{nj}^{\ell}(x)$  is a generalization of the hypergeometric function. Most previous attempts to solve this problem have involved approximations that ignore the contribution of the real function  $R_{nj}^{\ell}$ . It was interesting to learn that if one attempted to evaluate this contribution to  $M_{nj}$  as a power series in  $p/k$  (Rayleigh's approximation) then every term of the expansion vanished identically.

The set of equations (5) was solved numerically with the aid of the Argonne IBM-704 and the University of California (San Diego)

CDC-1604 computers. The technique was the standard one of starting with a  $1 \times 1$  matrix (the central element) and then increasing the size step by step until the values of the low-order reflection coefficients had "converged." A "goodness of solution" criterion was provided by computing the value of

$$\sum_l R_l \mu_l / \mu_0 . \quad (10)$$

Conservation of flux requires that this quantity have the value unity.

Figures 16-19 show the comparison between the experimental results of La Casce and Tamarkin<sup>2</sup> and the calculation described here. The general trend of agreement seems to be encouraging. Unfortunately, the nature and the description of the experiment are such that a detailed analysis of the extent of the agreement is not possible since no basis is yet available for discussing the precision or the necessity of corrections to the experiment.

I am indebted to

Dr. F. N. Spiess for the repeated hospitality of the Marine Physical Laboratory, and to Mr. R. Morell of Argonne for some of the programming.

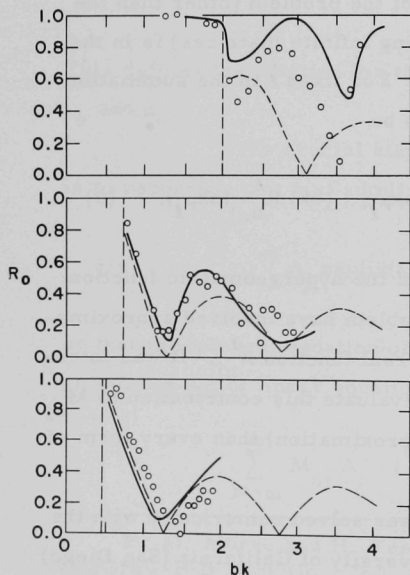


Fig. 16. The reflection coefficient  $R_0$  for normal incidence. The parameters of the reflecting surface are, from top to bottom,  $b = 0.32, 0.24,$  and  $0.15$  cm and  $p = 6.64, 3.12,$  and  $3.08$  cm<sup>-1</sup>. The dashed curve represents the predictions of Rayleigh's theory and is taken, along with the experimental points, from reference 2. The solid curve shows the present calculation.



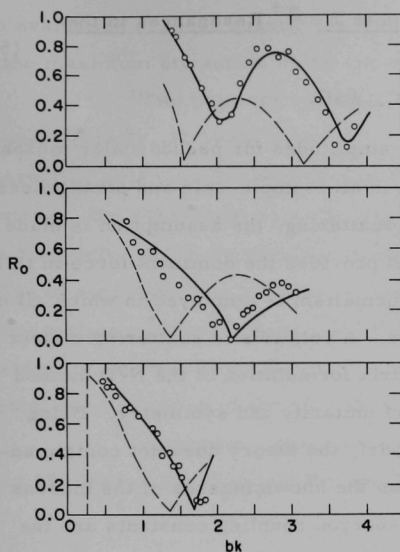


Fig. 17. The same as Fig. 16 except that the angle of incidence is  $40^\circ$  from the normal.

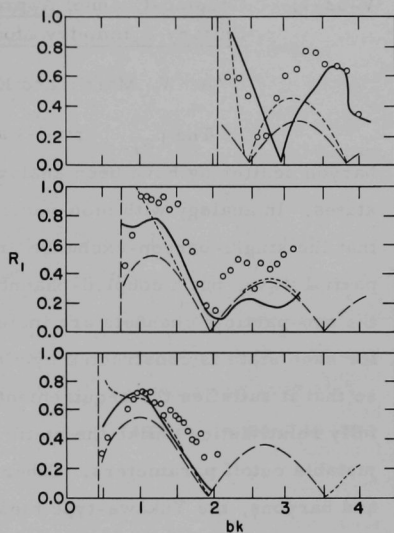


Fig. 18. The reflection coefficient  $R_1$  for normal incidence. The curves for the different values of parameters  $b$  and  $p$  are in the same orders as in Fig. 16. The short dashes are the predictions of Brekhovskikh, the long dashes those of Eckart. Both are copied from reference 2.

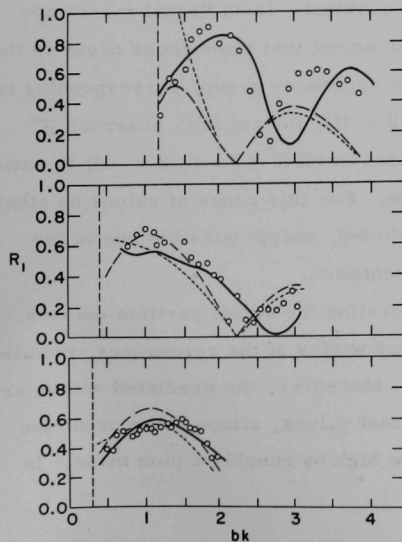


Fig. 19. The first-order backward reflection coefficient  $R_{-1}$  for  $40^\circ$  incidence. Otherwise the caption of Fig. 18 applies.

V-52-1. Coupled-Channel Approach to  $J = \frac{3}{2}^+$  Resonances in the Unitary-Symmetry Model (51151-01)

A. W. Martin and K. C. Wali

The  $P_{3/2}$  partial-wave amplitudes for pseudoscalar meson-baryon scattering have been analyzed in all isotopic-spin and strangeness states. In analogy with pion-nucleon scattering, the assumption is made that the single-baryon-exchange graph provides the dominant force in this partial wave, but a coupled-channel formalism is employed in which all of the two-particle channels are included. A relativistic scattering matrix for each state is constructed by a matrix formulation of the N/D method so that it satisfies the requirements of unitarity and symmetry. Being fully relativistic, unlike the static model, the theory does not contain adjustable cutoff parameters. Other than the known masses of the mesons and baryons, the Yukawa-type meson-baryon coupling constants are the only parameters that enter into the calculation.

The octet model of Gell-Mann and Ne'eman is used to define the coupling constants in terms of a single parameter  $f$  and the experimentally measured pion-nucleon coupling constant. In an "equal mass" approximation it is shown that the requirement that resonances occur in the ten-fold representation of the unitary-symmetry group, corresponding to the  $N^*$  ( $T = 3/2$ ,  $S = 0$ ),  $Y_1^*$  ( $T = 1$ ,  $S = -1$ ), the recently observed  $\Xi^*$  ( $T = 1/2$ ,  $S = -2$ ), and a yet-to-be-discovered  $Z^-$  ( $T = 0$ ,  $S = -3$ ), is satisfied by  $f$  in the range  $0.15 < f < 0.56$ . For this range of values no other resonances in the  $P_{3/2}$  state are predicted, except possibly one in the unitary singlet ( $T = 0$ ,  $S = -1$ ) representation.

It is found that incorporating the actual particle masses, in order to determine the locations and widths of the resonances, modifies the allowed range for  $f$  only slightly. Moreover, the predicted widths are in good agreement with the experimental values, although the predicted resonance locations are uniformly too high by roughly a pion mass. In

the evaluation of these quantities,  $f$  was taken to be  $1/4$ , which corresponds to the maximum attraction in the ten-fold representation in this model.

Two primary conclusions can be drawn from these considerations. Firstly, no basic inconsistency in the octet model of the strongly interacting particles has emerged in this dynamical calculation. On the contrary, the agreement with experiment is surprisingly good in view of the simplicity of the dynamic model employed. Secondly, the limited range of acceptable values of the parameter  $f$  predicts values of the Yukawa-type coupling constants which may be checked experimentally. An additional question of interest from the point of view of the octet model is the experimental determination of the spin-parity of the  $Y_0^*$  resonance at 1405 MeV.

A complete description of the calculation will appear in the June 15 issue of the Physical Review.

The evaluation of the model is based on the results of the comparison of the model with the experimental data. The model is considered to be valid if the results of the comparison are satisfactory.

Two types of results can be obtained from the comparison. Firstly, the results of the comparison can be used to check the validity of the model.

Secondly, the results of the comparison can be used to check the validity of the model. The results of the comparison can be used to check the validity of the model.

The results of the comparison can be used to check the validity of the model. The results of the comparison can be used to check the validity of the model.

The results of the comparison can be used to check the validity of the model. The results of the comparison can be used to check the validity of the model.

The results of the comparison can be used to check the validity of the model. The results of the comparison can be used to check the validity of the model.

The results of the comparison can be used to check the validity of the model. The results of the comparison can be used to check the validity of the model.

The results of the comparison can be used to check the validity of the model. The results of the comparison can be used to check the validity of the model.

The results of the comparison can be used to check the validity of the model. The results of the comparison can be used to check the validity of the model.

The results of the comparison can be used to check the validity of the model. The results of the comparison can be used to check the validity of the model.

The results of the comparison can be used to check the validity of the model. The results of the comparison can be used to check the validity of the model.

The results of the comparison can be used to check the validity of the model. The results of the comparison can be used to check the validity of the model.

The results of the comparison can be used to check the validity of the model. The results of the comparison can be used to check the validity of the model.

The results of the comparison can be used to check the validity of the model. The results of the comparison can be used to check the validity of the model.

The results of the comparison can be used to check the validity of the model. The results of the comparison can be used to check the validity of the model.

# PUBLICATIONS SINCE THE LAST REPORT

## PAPERS

### POSSIBLE THREE-PHONON GROUP FROM $\text{Ni}^{62}$

H. W. Broek . . . . . (Project I-22)  
Phys. Letters 3 (3), 132-134 (December 15, 1962)

### PARTICLES WITH ZERO MASS AND PARTICLES WITH "SMALL" MASS

F. Coester . . . . . (Project V-38)  
Phys. Rev. 129, 2816-2817 (15 March 1963)

### THE DEFORMATION ENERGY OF A CHARGED DROP. IV. EVIDENCE FOR A DISCONTINUITY IN THE CONVENTIONAL FAMILY OF SADDLE POINT SHAPES

S. Cohen and W. J. Swiatecki . . . . . (Project V-1)  
Ann. Phys. (New York) 19, 67-164 (July 1962)

### RATIO OF SYMMETRIC TO ASYMMETRIC FISSION FOR RESONANCE-NEUTRON FISSION OF $\text{U}^{235}$

L. E. Glendenin (CHM), K. F. Flynn (CHM), and L. M. Bollinger . . . . . (Project I-3)  
Trans. Am. Nuclear Soc. 5 (1), 20-21 (June 1962)

### BERYLLIUM WINDOW FOR GAMMA RAYS IN A LIQUID-HELIUM CRYOSTAT

J. Heberle . . . . . (Project I-19)  
Rev. Sci. Instr. 33, 1476-1477 (December 1962)

### THREE-NEUTRINO HYPOTHESIS

K. Hiida . . . . . (Project V-47)  
Nuovo cimento 27, 1439-1449 (1963)

### $\Sigma$ BREAKUP AND THE $\Sigma\Lambda$ RELATIVE PARITY

K. Hiida, J. L. Uretsky, and R. J. Oakes . . . (Project V-47)  
Nuovo cimento 27, 1262-1265 (1 March 1963)

### ÜBER EIN MASSENSPEKTROMETER ZUM NACHWEIS GEPULSTER MOLEKULARSTRAHLEN UND SEINE VERWENDUNG ZUR UNTERSUCHUNG VON ADSORPTIONS- UND DESORPTIONSVORGÄNGEN AN METALLOBERFLÄCHEN

M. S. Kaminsky . . . . . (Project II-22)  
Phys. Verh. VDPG 1, 66 (1961)

# A TEST OF THE STATISTICAL NATURE OF FLUCTUATIONS IN NUCLEAR CROSS SECTIONS

L. L. Lee, Jr., and J. P. Schiffer . . . . . (Project I-31)  
Phys. Letters 4, 104-105 (15 March 1963)

# REGGE TRAJECTORY IN FIELD THEORY

L. S. Liu and K. Tanaka . . . . . (Project V-45)  
Phys. Rev. 129, 1876-1879 (February 15, 1963)

# MEASUREMENTS OF LIFETIMES OF RADIOACTIVE SOURCES

J. E. Monahan, S. Raboy, and C. C. Trail . . . (Project I-55)  
Nuclear Instr. and Methods 17 (3), 225-230 (December 1962)

# MASS SPECTRA RESULTING FROM HIGH-ENERGY ELECTRON IMPACT ON SOME HYDROCARBON MOLECULES

J. E. Monahan and H. E. Stanton . . . . . (Project II-40)  
J. Chem. Phys. 37, 2654-2661 (December 1, 1962)

# POSSIBLE DETERMINATION OF THE SPIN OF THE $\Xi^-$ FROM THE ANGULAR ASYMMETRY OF ITS DECAY

M. Peshkin . . . . . (Project V-5)  
Phys. Rev. 129, 1864-1866 (15 February 1963)

# (n,2n) REACTION CROSS SECTIONS FROM 12 TO 19.6 MEV

L. A. Rayburn . . . . . (Project I-90)  
Phys. Rev. 130, 731-734 (15 April 1963)

# 3.86-MEV LEVEL IN $F^{17}$ . . . . . (Project I-21)

R. E. Segel, P. P. Singh, R. G. Allas, and S. S. Hanna  
Phys. Rev. Letters 10, 345-347 (15 April 1963)

# GAMMA-RAY SPECTRUM FROM THERMAL-NEUTRON CAPTURE IN $Hf^{177}$ AND ASSOCIATED ENERGY LEVELS IN $Hf^{178}$

R. K. Smither . . . . . (Project I-60)  
Phys. Rev. 129, 1691-1708 (15 February 1963)

# NEUTRAL SCALAR $\sigma$ MESON AND THE MASS DIFFERENCE BETWEEN MUON AND ELECTRON

K. Tanaka . . . . . (Project V-45)  
Nuovo cimento 21, 169-176 (1 July 1961)

# TEMPERATURE AND CARATHÉODORY'S TREATMENT OF THERMODYNAMICS

L. A. Turner (LDO) . . . . . (Unattached)  
J. Chem. Phys. 38, 1163-1167 (1 March 1963)

THE EFFECT OF TARGET THICKNESS AND BEAM STRAGGLING ON  
THE MAGNITUDE OF RESONANCES IN ELASTIC SCATTERING EX-  
PERIMENTS

J. A. Weinman . . . . . (Project I-21)  
Nuclear Instr. and Methods 21, 181-182 (1963)

ON THE MECHANISM OF THE ISOTOPIC EXCHANGE OF TRITIUM  
WITH METHANE

S. Wexler . . . . . (Project II-41)  
J. Am. Chem. Soc. 85, 272-277 (February 5, 1963)

ABSTRACTS

THE REACTION OF GRAPHITE WITH NITROGEN AT ELEVATED  
TEMPERATURES

J. Berkowitz . . . . . (Project II-29)  
Proceedings of the IAEA Symposium on Thermodynamics  
of Nuclear Materials, Vienna, May 21-25, 1962 (Inter-  
national Atomic Energy Agency, Vienna, 1962), pp. 505-516

Proceedings of the Midwest Conference on Theoretical Physics, Argonne  
National Laboratory, June 1-2, 1962

GEOMETRIC THEORY OF CHARGE AND BARYON NUMBER

H. Ekstein . . . . . (Project V-42)  
pp. 115-119

ON THE "REALITY" OF THE ELECTROMAGNETIC VECTOR POTENTIAL

M. Peshkin . . . . . (Project V-33)  
pp. 1-13

St. Louis meeting of the American Physical Society, March 25-28, 1963

BCS DESCRIPTION OF THE SUPERCURRENT STATE

M. Peshkin . . . . . (Project V-33)  
Bull. Am. Phys. Soc. 8, 191 (25-28 March 1963)

BROWNIAN MOTION OF HAMILTONIAN MATRICES

N. Rosenzweig . . . . . (Project V-15)  
Bull. Am. Phys. Soc. 8, 263 (25-28 March 1963)



Washington, D. C. meeting of the American Physical Society, April 22-25, 1963

# FISSION CROSS SECTION OF $\text{Th}^{229}$ FOR SLOW NEUTRONS

L. M. Bollinger, H. Diamond, and J. E. Gindler. .(Project I-3)  
Bull. Am. Phys. Soc. 8, 370 (April 22-25, 1963)

# COLLECTIVE LEVELS IN ZIRCONIUM ISOTOPES

H. W. Broek . . . . . (Project I-22)  
Bull. Am. Phys. Soc. 8, 376 (April 22-25, 1963)

# LIFETIME OF THE FIRST EXCITED STATE IN $\text{Ca}^{41}$ AT 1.95 MEV

C. M. Class, P. P. Singh, and S. S. Hanna . . . (Project I-21)  
Bull. Am. Phys. Soc. 8, 358 (April 22-25, 1963)

# NEUTRON RESONANCES IN SELENIUM . . . . . (Project I-3)

R. E. Coté, L. M. Bollinger, and G. E. Thomas  
Bull. Am. Phys. Soc. 8, 334 (April 22-25, 1963)

# p-WAVE NEUTRON CAPTURE IN Zr, Mo, AND Nb

H. E. Jackson . . . . . (Project I-7)  
Bull. Am. Phys. Soc. 8, 376 (April 22-25, 1963)

# MÖSSBAUER EFFECT OF $\text{Fe}^{57}$ IN HEXAGONAL COBALT

C. E. Johnson, G. J. Perlow, and W. Marshall. . (Project I-19)  
Bull. Am. Phys. Soc. 8, 351 (April 22-25, 1963)

# X RAYS FROM MU-MESONIC ATOMS

C. S. Johnson, H. L. Anderson, E. P. Hincks, S. Raboy,  
and C. C. Trail . . . . . (Project I-55)  
Bull. Am. Phys. Soc. 8, 324 (April 22-25, 1963)

# INTERACTION BETWEEN ION BEAMS AND METAL SINGLE-CRYSTAL SURFACES IN THE RUTHERFORD COLLISION REGION

M. S. Kaminsky . . . . . (Project II-23)  
Bull. Am. Phys. Soc. 8, 338-339 (April 22-25, 1963)

# ON THE STATISTICAL NATURE OF FLUCTUATIONS IN NUCLEAR CROSS SECTIONS

L. L. Lee, Jr., and J. P. Schiffer . . . . . (Project I-31)  
Bull. Am. Phys. Soc. 8, 375 (April 22-25, 1963)

# ELASTIC SCATTERING OF PROTONS BY $\text{Mg}^{26}$

M. C. Mertz . . . . . (Project I-31)  
Bull. Am. Phys. Soc. 8, 318 (April 22-25, 1963)

Washington, D.C. meeting of the American Physical Society, April 22-25, 1963 (cont'd.)

#### CAPTURE GAMMA RAYS FROM $\text{Ca}^{44}$

S. Raboy and C. C. Trail . . . . . (Project I-55)  
Bull. Am. Phys. Soc. 8, 358 (April 22-25, 1963)

#### ELASTIC AND INELASTIC SCATTERING FROM Ni ISOTOPES

J. P. Schiffer and L. L. Lee, Jr. . . . . (Project I-31)  
Bull. Am. Phys. Soc. 8, 375 (April 22-25, 1963)

#### PION-PION SCATTERING FROM A LAGRANGIAN VIEWPOINT

K. Smith (AMD) and J. L. Uretsky . . . . . (Project V-49)  
Bull. Am. Phys. Soc. 8, 300 (April 22-25, 1963)

#### TOTAL CROSS SECTION OF $\text{Th}^{232}$ FOR SLOW NEUTRONS

G. E. Thomas and L. M. Bollinger . . . . . (Project I-3)  
Bull. Am. Phys. Soc. 8, 334 (April 22-25, 1963)

### ANL TOPICAL REPORTS

#### BENDING-MAGNET AND QUADRUPOLE ABERRATIONS FOR PARAXIAL RAYS

M. L. Good . . . . . (Unattached)  
Argonne National Laboratory Topical Report ANL-6611  
(November 1962)

#### HANDBOOK FOR THE NANOSECOND ELECTRON ACCELERATOR (NSEA)

E. A. Mroz, W. L. Buck, R. K. Swank, and H. B. Phillips . . . . . (Project I-144)  
Argonne National Laboratory Topical Report ANL-6700  
(March 1963)

### ACM STUDENT REPORT

#### NUCLEAR ZEEMAN EFFECT OF THE 23.8-KEV GAMMA RAY OF $\text{Sn}^{119}$

M. Pronga . . . . . (Project I-19)  
ACM student report to Monmouth College (February 1963)

## CO-OP STUDENT REPORT

TESTING A MODEL OF THE NUCLEAR POTENTIAL—A STUDENT'S  
VIEW OF A PROBLEM

D. J. Mueller . . . . . (Project I-18)  
Co-op student report to Northwestern University (March 25,  
1963)

# ADDITIONAL PAPERS ACCEPTED FOR PUBLICATION

## COLLECTIVE EXCITATIONS IN $Ni^{58,60,62}$ AND $Zn^{64,66,68}$

H. W. Broek . . . . . (Project I-22)  
Phys. Rev. (May 15, 1963)

## NONLEPTONIC DECAYS OF HYPERONS

S. N. Gupta . . . . . (Unattached)  
Phys. Rev.

## PHASE RELATION IN NUCLEAR SCATTERING

D. R. Inglis . . . . . (Project V-3)  
Nuclear Phys.

## ATOMIC AND IONIC IMPACT PHENOMENA ON METAL SURFACES

M. S. Kaminsky . . . . . (Project II-23)  
Monograph in the series "Struktur und Eigenschaften der  
Materie" (Springer Verlag, Berlin)

## A PULSED-MOLECULAR-BEAM MASS SPECTROMETER FOR STUDIES OF ATOMIC AND IONIC IMPACT PHENOMENA ON METAL SURFACES

M. S. Kaminsky . . . . . (Project II-22)  
Advanced Energy Conversion (Pergamon Press, New York)

## STRONG M1 TRANSITIONS IN LIGHT NUCLEI

D. Kurath . . . . . (Project V-8)  
Phys. Rev. (May 15, 1963)

## INTERMEDIATE COUPLING

D. Kurath . . . . . (Unattached)  
Beta and Gamma Ray Spectroscopy, edited by K. Siegbahn  
(Interscience Publishers, Inc., New York), second edition

## ON THE INTERFERENCE OF LINEARLY POLARIZED LIGHT WITH PERPENDICULAR POLARIZATIONS

A. Langsdorf, Jr. . . . . (Unattached)  
Am. J. Phys. (August or September 1963)

## COUPLED CHANNEL APPROACH TO $J = \frac{3}{2}^+$ RESONANCES IN THE UNITARY SYMMETRY MODEL

A. W. Martin and K. C. Wali . . . . . (Project V-52)  
Phys. Rev. (June 15, 1963)

# CALCULATION OF DEUTERON STRIPPING AMPLITUDES USING S-MATRIX REDUCTION TECHNIQUES

A. M. Saperstein . . . . . (Project V-11)  
Phys. Rev. (June 1, 1963)

## PROTON WIDTHS IN A DIFFUSE WELL

J. P. Schiffer . . . . . (Project I-30)  
Nuclear Phys. (June 1963)

## THE OBSERVATION OF $\text{Be}^8$ IN THE GROUND STATE

J. A. Weinman and R. K. Smither . . . . . (Project I-21)  
Nuclear Phys. 43 (1963)

## IONIZATION BY IONS IN THE MEV RANGE

S. Wexler and D. C. Hess . . . . . (Project II-31)  
J. Chem. Phys. (May 1963)

PERSONNEL CHANGES IN THE ANL PHYSICS DIVISION

## NEW MEMBERS OF THE DIVISION

Resident Research Associates

Dr. Bhalchandra M. Udgaonkar, Tata Institute of Fundamental Research, Bombay, India. Bootstrap calculations of resonances and bound states. Came to Argonne on April 22, 1963. (Host: M. Peshkin.)

Student Aide (Co-op)

Mr. Brent Blumenstein, University of Florida. Working with R. O. Lane on analysis of data on neutron scattering. Came to ANL on April 29, 1963.

Technician

Mr. Ralph Waldhauser joined the Physics Division on April 26, 1963 as a Research Technician (Junior) to work with Jack Wallace.

Secretary

Mrs. Margaret Isom returned to the Physics Division on March 1, 1963 as the Physics Division secretary.

## DEPARTURES

Dr. Charles E. Johnson, resident research associate, has been at Argonne since September 10, 1962. He collaborated with G. J. Perlow on the Mössbauer effect. He terminated at ANL on April 16, 1963 to return to A.E.R.E., Harwell, England.

Dr. James A. Weinman, associate physicist, has been at Argonne since January 18, 1960. He has worked on the excited states of light nuclei (Project I-21), mostly at the 4.5-MeV Van de Graaff. He terminated at ANL on March 15, 1963 to go to the Department of Meteorology, University of Wisconsin, Madison 6, Wisconsin.

## TRANSFERS

Mr. Charles Perko has transferred to Central Shops. He left the Physics Division on February 18, 1963.

Mrs. Catherine Yack transferred to LDO on March 1, 1963 to continue as secretary to Dr. Morton Hamermesh.



ARGONNE NATIONAL LAB WEST



3 4444 0008857 5